Self-Assembly of Bilayers from Double-Chain Fluorocarbon Amphiphiles in Aprotic Organic Solvents: Thermodynamic Origin and Generalization of the Bilayer Assembly

Yuichi Ishikawa,[†] Hiroaki Kuwahara, and Toyoki Kunitake*

Contribution No. 986 from the Department of Chemical Science and Technology, Faculty of Engineering, Kyushu University, Hakozaki, Higashi-ku, Fukuoka 812, Japan

Received November 1, 1993[●]

Abstract: We designed new fluorocarbon amphiphiles, 3–7, that undergo spontaneous bilayer formation in organic media. They are comprized of double fluorocarbon chains and a single oleyl chain as solvophobic and solovophilic moieties, respectively. These two molecular modules were linked through the chiral L-glutamate residue. When dispersed in chlorocyclohexane or benzene, these amphiphiles formed stable bilayer assemblies that gave rise to morphologies such as tubes, tapes, rods, and particles as confirmed by electron microscopy. These dispersions showed bilayer/monomer phase transitions as inferred by differential scanning calorimetry. This phase transition was accompanied by changes of the helical pitch of the fluorocarbon conformation and of intermolecular hydrogen bonding among the glutamate moiety. From the surface tension analysis of adsorbed monolayers at the air/liquid interface, we concluded that the bilayer formation in bulk chlorocyclohexane was driven by the enthalpic change. Limited miscibilities between fluorocarbon chains and hydrocarbon solvents produced the main enthalpic driving force of the molecular association, and the hydrogen bonding and van der Waals force of the aromatic moieties served as secondary driving forces. The molar fraction at CMC (critical membrane or micelle concentration), which reflects instability of aggregates, was greater than those of aqueous bilayers (below 10^{-7}) but smaller than those of aqueous micelles (above 10^{-4}). The chromophoric bilayers 6 (Phe-Ole) and 7 (Azo-Ole) showed large molecular ellipticities of 10^5–10^6 deg·cm^2·dmol^{-1} in their CD spectra. Molecular ordering in the novel bilayers was not inferior to those of conventional aqueous bilayers, although their bilayer stability does not surpass that of aqueous bilayers.

Introduction

Molecular design of "amphiphiles" has been carried out by assuming the use of "water" as the solvent. This is because the hydrophobic force is considered to be indispensable for efficient assembly of amphiphiles. It is true that conventional surfactants such as alkylammonium salts can form micelles even in non-aqueous, protic environments such as hydrazine,[1–3] formamides,[4–10] glycols,[11] glycerols,[12] and ethylammonium nitrate (a low-melting fused salt).[13] However, their CMC's in these media are markedly higher and the corresponding aggregate numbers are much smaller than those of aqueous micelles.[1–13] It is clear that sufficiently stable aggregates are not obtainable in nonaqueous media from conventional amphiphilic compounds.[14]

Our objective in this research is to find design principles for bilayer assembly in aprotic organic media. Through synthesis and characterization of hundreds of bilayer-forming amphiphiles, we have proposed a generalized molecular design of aqueous bilayer membranes.[15,16] If these design principles could be modified so as to encompass aprotic, non-water-like media, a novel rich field of molecular assembly would emerge. In order to realize stable assemblies in aprotic organic media, it is essential to use molecular assembling forces that are comparable in strength to the hydrophobic force in the aqueous system.

Long perfluoroalkyl compounds generally display low solubilities in hydrocarbon media due to their small cohesive forces.[17] Thus, perfluoroalkyl chains in the liquid state are forced to remain assembled by hydrocarbon surroundings. This unique property has been incorporated into aqueous bilayer membranes. Ammonium amphiphiles possessing perfluoroalkyl chains in place of hydrocarbon chains can form stable, well-aligned aqueous bilayers (**1** vs **2**).[16,18–21] These fluorocarbon bilayers tend to phase-separate (cluster formation) when mixed with hydrocarbon bilayers,[18–21] as is the case with aqueous micelles.[22] It is reported that a half-fluorinated bolaamphiphile forms an asymmetric monolayer

---

[†] Current address: Department of Applied Chemistry, Faculty of Engineering, Oita University, Dannobaru 700, Oita 870-11, Japan.

[●] Abstract published in *Advance ACS Abstracts,* June 1, 1994.

(1) Evans, D. F. *Langmuir* **1988**, *4*, 3–12.

(2) Ramadan, M. Sh.; Evans, D. F.; Lumry, R. *J. Phys. Chem.* **1983**, *87*, 4538–4543.

(3) Ramadan, M. Sh.; Evans, D. F.; Lumry, R.; Philson, S. *J. Phys. Chem.* **1985**, *89*, 3405–3408.

(4) Rico, I.; Lattes, A. *J. Phys. Chem.* **1986**, *90*, 5870–5872.

(5) Belmajdoub, A.; ElBayed, K.; Brondeau, J.; Canet, D.; Rico, I. *J. Phys. Chem.* **1988**, *92*, 3569–3573.

(6) Auvray, X.; Petipas, C.; Anthore, R.; Rico, I. Lattes, A. *J. Phys. Chem.* **1989**, *93*, 7458–7464.

(7) Sjoberg, M.; Silveston, R.; Kronberg, B. *Langmuir* **1993**, *9*, 937–979.

(8) Jonstromer, M.; Sjoberg, M.; Warnheim, T. *J. Phys. Chem.* **1990**, *94*, 7549–7555.

(9) Sjoberg, M.; Jansson, M.; Henriksson, U. *Langmuir* **1992**, *8*, 409–413.

(10) Singh, H. N.; Saleem, S. M.; Singh, R. P.; Birdi, K. S. *J. Phys. Chem.* **1980**, *84*, 2191–2194.

(11) Ray, A. *J. Am. Chem. Soc.* **1969**, *91*, 6511–6512.

(12) Fletcher, D. P. I.; Gilbert, P. J. *J. Chem. Soc., Faraday Trans. 1,* **1989**, *85*, 147–156.

(13) Evans, D. F.; Yamauchi, A.; Wel, G. J.; Bloomfield, V. A. *J. Phys. Chem.* **1983**, *87*, 3537–3541.

(14) However, it is possible to obtain regular, stable gel assemblies in aromatic media by introducing multiple hydrogen bonds such as polyamides: Ihara, H.; Hachisako, H.; Hirayama, C.; Yamada, K. *J. Chem. Soc., Chem. Commun.* **1992**, 244–1245. Fuhrhop, J.-H.; Schnieder, P.; Boekema, E.; Helfrich, W. *J. Am. Chem. Soc.* **1988**, *110*, 2861–2867.

(15) Kunitake, T.; Ando, R.; Ishikawa, Y. *Mem. Fac. Eng. Kyushu Univ.* **1986**, *46*, 221–263. Kim, J.-M.; Kunitake, T. *Ibid.* **1989**, *49*, 93–108.

(16) Kunitake, T. *Angew. Chem., Int. Ed. Engl.* **1992**, *31*, 709–726.

(17) Fluorocarbons have the lowest surface energies. For instance, the surface tension of perfluoro-*n*-hexane is 11.4 mN/m: Stiles, V. E.; Cady, G. H. *J. Am. Chem. Soc.* **1952**, *74*, 3771–3773. Moreover, perfluorooctanesulfonamide derivatives reduce the surface tension of water to about 7 mN/m: Kimura, C.; Murai, K.; Kashiwaya, K.; Takahashi, H.; Nishiyama, T. *J. Jpn. Oil Chem. Soc.* **1982**, *31*, 448–451.

(18) Kunitake, T.; Okahata, Y.; Yasunami, S. *J. Am. Chem. Soc.* **1982**, *104*, 5547–5549.

(19) Kunitake, T.; Higashi, N. *J. Am. Chem. Soc.* **1985**, *107*, 692–696.

(20) Elbert, R.; Folda, T.; Ringsdorf, H. *J. Am. Chem. Soc.* **1984**, *106*, 7687–7692.

(21) Trabelsi, H.; Szonyi, S.; Gaysinski, M.; Cambon, A. Watzke, H. J. *Langmuir* **1993**, *9*, 1201–1205.

(22) See, for a recent example: Caponetti, E.; Martino, D. C.; Floriano, M. A.; Triolo, R. *Langmuir* **1993**, *9*, 1193–1200.

0002-7863/94/1516-5579$04.50/0

Chart 1

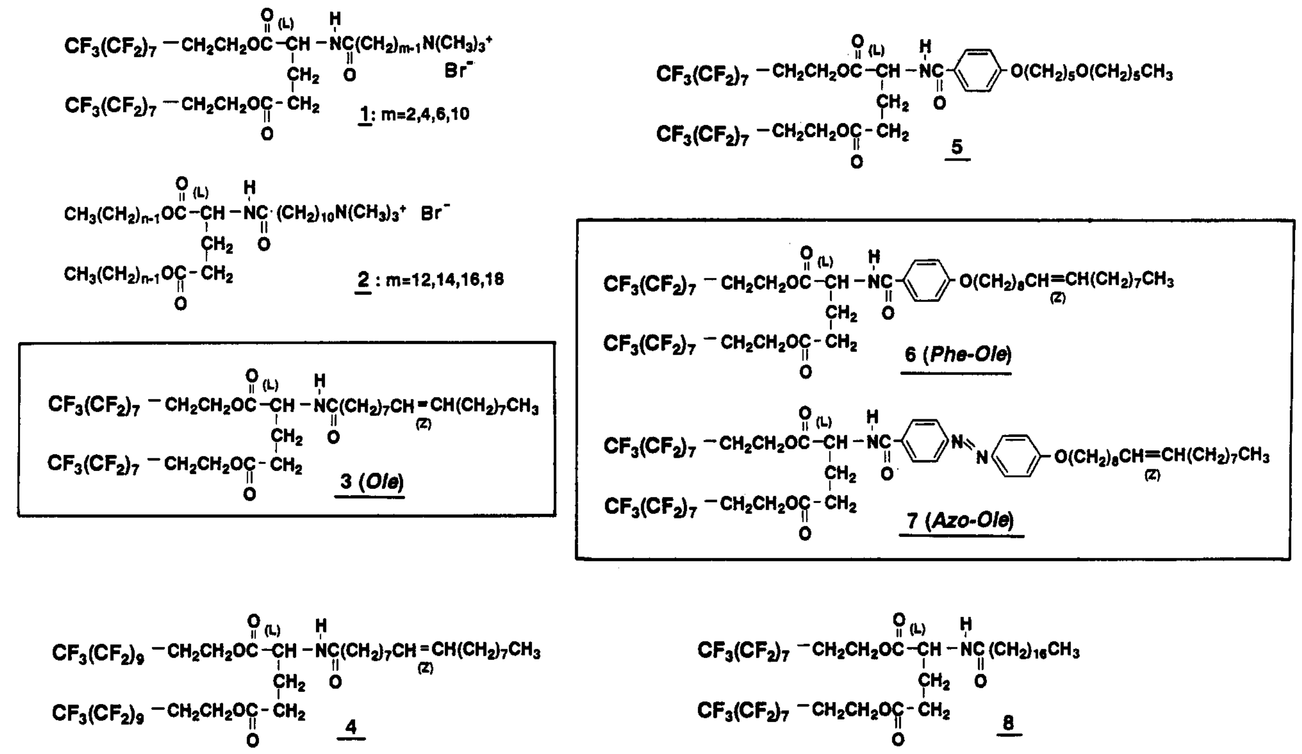

vesicle in water due to hydrocarbon/fluorcarbon phase separation.[23] The limited miscibility has been noticed also at the air/hydrocarbon interface. Long perfluoroalkyl chains linked with the hydrocarbon moiety form insoluble monolayer films[24] and reduce surface tension.[25-30] Their spreading onto organic surfaces can be controlled by the ratio of the organophobic/organophilic portions of solutes.[26]

On the basis of these precedents, we designed the first example of stable bilayer assemblies formed in aprotic, organic media such as cyclohexane, benzene, and 2-butanone from fluorocarbon/hydrocarbon amphiphiles, **3**, **4**, and **5**, and described their aggregation behavior briefly.[31] Turberg and Brady separately reported that semi-fluorinated alkanes, C_8F_{17}–C_nH_{2m+1} (m = 12, 16), assembled into micellar aggregates in toluene and perfluorooctane.[32]

In order to carry out a systematic examination of the structure–aggregation relation in aprotic, organic media, we selected a series of fluorocarbon/hydrocarbon amphiphiles, **3**(Ole), **6**(Phe-Ole), and **7**(Azo-Ole), in this research and examined their bilayer behavior. In particular, the thermodynamic aspect of aggregation was carefully studied to elucidate the driving force of the self-assembly.

Results and Discussion

1. Molecular Design. In order to realize bilayer assembly in hydrocarbon solvents, we synthesized six fluorocarbon amphiphiles, **3–8**, shown in Chart 1. These compounds are composed of the following four molecular modules: (1) double fluorocarbon chains as the solvophobic portion, (2) the glutamate connector that is chiral and is capable of hydrogen bonding, (3) an aromatic unit next to the connector module as chromophoric reporter and a supplier of the van der Waals force, and (4) a flexible hydrocarbon chain as the solvophilic module. We avoided the use of a single solvophobic chain in favor of the double fluorocarbon chains in order to acquire sufficient solvophobicity and to promote molecular alignment, since single-chained semifluorocarbons give fluid micellar assemblies or molecular dispersion.[30,32] It is readily anticipated that the increase in the length of the fluorocarbon chain enhances the driving force for aggregation. For instance, the use of fluorocarbon chains longer than perfluorooctyl is essential to cause phase separation (domain formation) of fluorocarbon components in $C_nF_{2n+1}COO^-/C_{12}H_{25}SO_4^-$ mixed micelles.[33] However, when we used perfluorodecyl derivative **4** in place of perfluorooctyl derivative **3**, sufficient solubility was not observed except in ketones.[34] On the basis of these facts, we were obliged to use the perfluorooctyl chain as the solvophobic module. The chiral L-glutamate residue was selected as a connector that links fluoroalkyl chains and the oleyl unit, since it has been effectively utilized in the design of aqueous bilayer-forming amphiphiles, e.g., **1** and **2**.[16,35,36] The amide unit and the aromatic chromophores included in the connector and spacer portions strengthen attractive molecular interactions. In fact, the influence of the latter unit is reflected in increasingly higher melting points with increasing sizes of the aromatic chromophore: mp 67 °C (**3** (Ole)), 92 °C (**6** (Phe-Ole)), and 137 °C (**7** (Azo-Ole)). The chromophores that are located close to the chiral carbon are instrumental in monitoring the molecular orientation by circular dichroism.

---

(23) Liang, K.; Hui, Y. *J. Am. Chem. Soc.* **1992**, *114*, 6588–6590.
(24) Ellison, A. H.; Zisman, W. A. *J. Phys. Chem.* **1955**, *59*, 1233.
(25) Scholberg, H. M.; Guenthner, R. A. *J. Phys. Chem.* **1953**, *57*, 923–925.
(26) Jarvis, N. L.; Zisman, W. A. *J. Phys. Chem.* **1959**, *63*, 727–734.
(27) Le Grand, D. G.; Gaines, G. L., Jr. *J. Colloid Interface Sci.* **1975**, *50*, 272–279.
(28) Katritzky, A. R.; Davis, T. L.; Rewcastle, G. W.; Rubel, G. O.; Pike, M. T. *J. Phys. Chem.* **1988**, *4*, 732–735.
(29) Abe, M.; Morikawa, K.; Ogino, K. *Langmuir* **1992**, *8*, 763–764.
(30) Gaines, G. J., Jr. *Langmuir* **1991**, *7*, 3054–3056.
(31) Ishikawa, Y.; Kuwahara, H.; Kunitake T. *J. Am. Chem. Soc.* **1989**, *111*, 8530–8531. Ishikawa, Y.; Kuwahara, H.; Kunitake, T. *Chem. Lett.* **1989**, 1737–1740.
(32) Turberg, M. P.; Brady, J. E. *J. Am. Chem. Soc.* **1988**, *110*, 7797–7801.
(33) Shinoda, K.; Nomura, T. *J. Phys. Chem.* **1980**, *84*, 365–369. Carlfors, J.; Stilbs, P. *J. Phys. Chem.* **1984**, *88*, 4410–4414.
(34) Unpublished results in these laboratories.
(35) Nakashima, N.; Asakuma, S.; Kim, J.-M.; Kunitake, T. *Chem. Lett.* **1984**, 1709–1712. Ishikawa, Y.; Nishimi, T.; Kunitake, T. *Chem. Lett.* **1990**, 25–28. Kimizuka, N.; Ohira, H.; Tanaka, M. *Chem. Lett.* **1990**, 29–32.
(36) Kunitake, T.; Tawaki, S.; Nakashima, N. *Bull. Chem. Soc. Jpn.* **1983**, *56*, 3235–3242.

Table 1. Dissolution Behavior[a] of **3** (Ole), **6** (Phe-Ole), **7** (Azo-Ole), **4**, **5**, and **8** at ca. 20 °C

	amphiphile					
medium	**3** (Ole) (1 mM)	**6** (Phe-Ole) (1 mM)	**7** (Azo-Ole) (0.1 mM)	**4** (1 mM)	**5** (0.1 mM)	**8** (1 mM)
aliphatic						
n-decane	G	C	C	C	C	C
cyclohexane	B	C	C	C	B	C
chlorocyclohexane	B	B	B	C		C
aromatic						
toluene	B	B	G (20 mM)	C	H	C
benzene	B	B	G (20 mM)	C	H	C
protic						
water	I	I	I	I	I	I
methanol	C	C	C	C	H	C
dipolar[a] protic						
dimethylformamide	C	C	C	C		C
halogenated						
CHCl$_3$	H	H	H	H	H	H
ketones/esters						
ethyl acetate	H	H	H	B	H	H
tetrahydrofuran	H	H	H	B		H
isopropyl ether	H	H	H			H

[a] All samples were heated to nearly their boiling points, then cooled to room temperature. Crystallization was confirmed by optical microscopic observation (magnification, ×200). Abbreviations: G, gelation; B, foaming clear solution; C, clear solution while hot, crystallization upon cooling; H, homogeneous clear solution; I, insoluble.

The solvophilic and solvophobic properties should be balanced in order to obtain stable dispersions. In the preliminary experiment, we chose the *n*-octadecyl chain as the solvophilic module as in **8**. This compound, however, showed insufficient solubilities (at 1 mM, 20 °C) in all solvents given in Table 1. Introduction of the flexible oleyl chain in place of the normal alkyl chain lowered melting point from 83 °C (**8**) to 62 °C (**3**(Ole)) and led to suitable solubilities in some of the solvents. The ether-linked flexible chain in **5** did not give dispersibility superior to that of the oleyl chain in **6** (Phe-Ole).

2. Selection of Solvent. The kind of organic solvent that serves our purpose is crucial particularly from the following two aspects, apart from general dispersibility. First, it is advisable not to select water-like organic solvents such as hydrazine,[1-3] formamide,[7] and polyols,[4,11,12] in order to demonstrate the generality of the self-organization process. This condition leads to a decisive demonstration that hydrogen bonding solvents are not a prerequisite for amphiphilic self-assembly.[1,37] Secondly, specific interactions between solute (amphiphiles) and solvent must be avoided.

In addition, both facile crystallization and molecular dissolution must be avoided. The use of volatile solvents will yield unreliable results in spectroscopic and surface chemical experiments. It is preferable to find common solvents for amphiphiles **3** (Ole), **6** (Phe-Ole), and **7** (Azo-Ole) in order to compare their self-assembly processes under identical conditions. We examined their dissolution processes in 41 solvents including those of Table 1. The presence of crystalline precipitates was confirmed by dark-field optical microscopy (×200 magnification).

Compounds **3** (Ole), **6** (Phe-Ole), and **7** (Azo-Ole) were hardly soluble in protic solvents, in dipolar aprotic solvents, and in normal alkanes, but they gave clear solutions in ester, ether, and halogenated alkane solvents even at room temperature. The amphiphiles could be dispersed in cyclic alkanes and aromatic solvents (chlorocyclohexane, toluene, and benzene) by heating. These dispersions were prone to foam by shaking, indicating the surface-active properties of these compounds. Therefore, these solvents were proper candidates for further examination.

The presence or absence of the aromatic group in **3** (Ole), **6** (Phe-Ole), and **7** (Azo-Ole) leads to different dissolution behaviors. While **6** (Phe-Ole) and **7** (Azo-Ole) (1 mM) gave clear solutions only in hot *n*-decane and cyclohexane (crystalline precipitates formed upon cooling), **3** (Ole) was dissolved in these solvents at room temperature. In contrast, **6** (Phe-Ole) and **7** (Azo-Ole) were more soluble than **3** (Ole) in aromatic solvents. Chlorocyclohexane dispersions of **6** (Phe-Ole) and **7** (Azo-Ole) gave crystalline precipitates above a certain concentration, but their dispersions in benzene and toluene were transformed into translucent gels with increasing concentrations. It is apparent that the aromatic units in **6** (Phe-Ole) and **7** (Azo-Ole) enhance their affinities toward aromatic solvents.

3. Aggregate morphology. Prior to physicochemical experiments, we studied the aggregate morphologies by optical and electron microscopies. Dark-field optical microscopy (magnification, ×200; room temperature) of dispersions of **3** (Ole), **6** (Phe-Ole), and **7** (Azo-Ole) (5 mM) in benzene and chlorocyclohexane displayed the presence of fibrous aggregates (length, 10^2 μm; diameter, 0.1 μm) that were stacked to yield huge rods or thicker fibers without regard to the molecular structures of these compounds (micrographs not shown).

Subsequently, transmisson electron microscopy (TEM) with negative staining was applied to these dispersions in order to observe morphologies at the molecular level. There was no information available for what kinds of dyes were suitable for negative staining in organic solvents. Thus, we conducted screening tests of the following oil-soluble heavy metal complexes as staining agents: HgCl$_2$, phenylmercury acetate, NMR shift reagents, and lead(II) bis(acetylacetonate). A hot methanol solution saturated with lead(II) bisacetylacetonate provided the best TEM contrast.[38] Direct staining of organic dispersions with this agent may cause considerable alteration of aggregate morphologies; hence, we adopted a post-staining method to minimize this detrimental effect.

Figure 1 shows TEM photographs of organic aggregates. The staining agent gives dark shadows. A chlorocyclohexane dispersion of **3** (Ole) (1 mM) contains oval structures of ca. 100-Å thickness and 200–2000-Å diameter (Figure 1a). On the other hand, a benzene dispersion of **3** (Ole) shows rods with 120-Å

---

(37) Beesley, A. H.; Evans, D. F.; Laughlin, R. G. *J. Phys. Chem.* **1988**, *92*, 791–793.

(38) Our recent attempt to improve the staining ability proved that lead(II) bis(dipivaloylmethanate) was superior to lead(II) bis(acetylacetonate).

(39) Kunitake, T.; Nakashima, N.; Shimomura, M.; Okahata, Y.; Kano, K.; Ogawa, T. *J. Am. Chem. Soc.* **1980**, *102*, 6642–6644. Nakashima, N.; Ando, R.; Fukushima, H.; Kunitake, T. *Chem. Lett.* **1985**, 1503–1506. Nakashima, N.; Morimitsu, K.; Kunitake, T. *Bull. Chem. Soc. Jpn.* **1984**, *57*, 3253–3257. Kunitake, T.; Kim, J.-M.; Ishikawa, Y. *J. Chem. Soc., Perkin Trans. 2* **1991**, 885–890.

(40) Nakashima, N.; Yamada, N.; Kunitake, T.; Umemura, J.; Takenaka, T. *J. Phys. Chem.* **1986**, *90*, 3374–3377.

(41) Kunitake, T.; Yamada, N.; Fukunaga, N. *Chem. Lett.* **1984**, 1089–1092. Kimizuka, N.; Kawasaki, T.; Kunitake, T. *J. Am. Chem. Soc.* **1993**, *115*, 4387–4388.

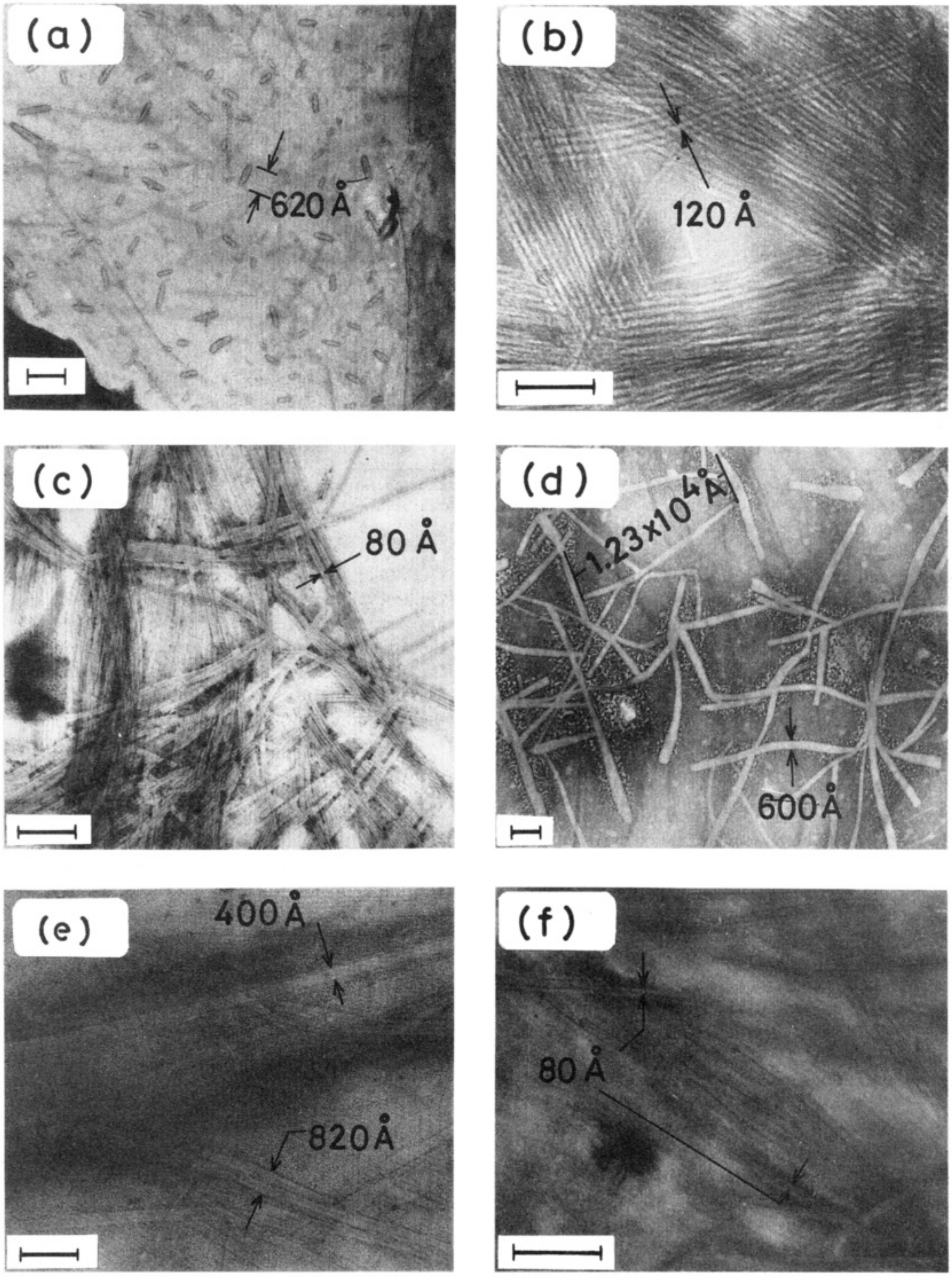

Figure 1. Transmission electron micrographs for **3** (Ole), **6** (Phe-Ole), and **7** (Azo-Ole) dispersed in organic solvents. Post-staining was performed with lead(II) bis(acetylacetonate) on carbon-coated TEM grids at about 10 °C. All scale bars represent 2000 Å. (a) Vesiclelike oval aggregates of **3** (Ole) (1 mM) in chlorocyclohexane, original magnification ×40 000. (b) Aligned rods of **3** (Ole) (1 mM) in benzene, original magnification ×80 000. (c) Stacked tubelike aggregates of **6** (Phe-Ole) (1 mM) in chlorocyclohexane, original magnification ×60 000. (d) Tapelike aggregates of **7** (Azo-Ole) (0.5 mM) in chlorocyclohexane, original magnification ×30 000. (e) The same sample as in d, original magnification ×60 000. (f) The same sample as in d, original magnification ×90 000.

thickness aligned with each other (Figure 1b). Compound **6** (Phe-Ole) in chlorocyclohexane (1 mM) formed clearly defined tubelike aggregates of 80-Å thickness (Figure 1c). Images of compound **7** (Azo-Ole) in chlorocyclohexane (0.5 mM) were visualized at three different magnifications: 30 000, 60 000 and 90 000. The lowest magnification shows tapelike aggregates of 10^3-Å width and 10^4-Å length (Figure 1d). At a higher magnification, we can see that the huge tape is made of a set of 3–8 stacked layers (Figure 1e) and that each layer is a tube of 80-Å thickness (Figure 1f). The narrowest part of these aggregates is about twice as thick as the molecular length (40–60 Å) of the component amphiphile, and the width of the other part of the assembly is roughly comparable to the several molecular layers. By combining this observation with the results of section 8, we conclude that these aggregates are not three-dimensional microcrystals or micellar dispersions. We reported previously that a related chiral fluorocarbon amphiphile, **5**, assembled into a helical tape of 1600-Å width and vesicles of 100-Å diameter in cyclohexane.[31]

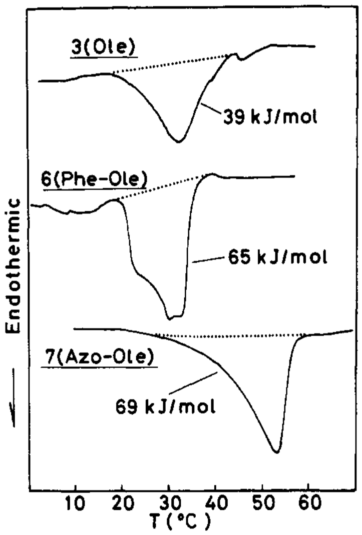

Figure 2. DSC thermograms of chlorocyclohexane dispersions (20 mM) of **3** (Ole), **6** (Phe-Ole), and **7** (Azo-Ole) (scanning rate, +1 °C/min).

Amphiphile **4** also gave bilayer-wide tapes of 10^3-Å length with twists. All the morphologies described in Figure 1 resemble those of aqueous chiral bilayers: tape, rod, helix, lamella, and vesicle.[16]

On the other hand, distinct aggregate morphologies could not be found at all in chloroform by microscopic observation. Considering the data of sections 6 and 7, it is obvious that **3** (Ole), **6** (Phe-Ole), and **7** (Azo-Ole) are dissolved in chloroform as monomeric species.

In the subsequent experiments, chlorocyclohexane was solely used as the solvent for the following reasons: (1) benzene and toluene are good solvents (see section 2), and the aggregate stability in these media is seemingly inferior to that in chlorocyclohexane; (2) CD spectral examination of molecular orientation is possible in this solvent; (3) surface tension measurements are reliable due to its high boiling point (141 °C).

4. Phase Transition Behavior. Aqueous bilayers have been known to show the "gel to liquid crystal" phase transition. It is one of the most fundamental membrane properties and gives rise to a variety of unique physicochemical changes. The phase transition behavior would provide invaluable information on the nature of these novel nonaqueous bilayers. Hence we examined the thermal behavior of chlorocyclohexane dispersions of **3** (Ole), **6** (Phe-Ole), and **7** (Azo-Ole) with differential scanning calorimetry (DSC).

Figure 2 represents DSC thermograms of chlorocyclohexane dispersions of **3** (Ole), **6** (Phe-Ole), and **7** (Azo-Ole) in the heating process. All the dispersions possess endothermic peaks which are reproducible during repeated scans. The endothermic peaks are located at 17–42 °C (peak top [pt] 32 °C, width at the half height [whh] 12 °C) for **3** (Ole), at 21–40 °C (pt 30 °C, whh 12 °C) for **6** (Phe-Ole), and at 27–57 °C (pt 53 °C, whh 10 °C) for **7** (Azo-Ole) with enthalpy changes of 40–70 kJ/mol. Related aqueous fluorocarbon bilayers, **1** (m = 2, 4, 6, 10), showed sharp (whh 1 °C) and small endothermic peaks (3–9 kJ/mol) at a high-temperature range of 84–95 °C.[15] The peaks of the nonaqueous bilayer are not so sharp, small, and high as those of analogous aqueous bilayers. The enthalpy change of the latter transition is 5–10 times larger than that of the former. We can infer from these thermal data that the phase transition in Figure 2 is inherently different from those of the ordinary aqueous bilayers. It is interesting to note that the enthalpy change of **3** (Ole), which has no aromatic module, is close to the sum of the heats of fusion of double perfluorooctyl chains and the cleavage energy of a hydrogen bond.[42]

In order to understand the nature of the phase transition, we measured molecular weights of **3** (Ole) and **7** (Azo-Ole) (2 mM) in chlorocyclohexane at 70 °C[44] (above the phase transition temperature) by vapor pressure osmometry. The observed molecular weights of **3** (Ole) and **7** (Azo-Ole) were 1.7×10^3 and 2.0×10^3, respectively. Both values are very close to those of the monomeric species. We conclude that the bilayer components are in the monomeric state at this temperature. The endothermic peaks in Figure 2, therefore, are ascribed to the "bilayer to monomer" conversion.

5. Molecular Orientation. Bilayer membranes are characterized by two-dimensional, regular molecular arrays. We have shown that exciton coupling is much enhanced among oriented chromophores in chiral aqueous bilayers. For instance, the chiral bilayers containing the phenylene or azobenzene chromophores gave rise to surprisingly large $[\theta]$ values ranging from 10^5 to 10^6 deg·cm^2·dmol^{-1} in the crystalline state in circular dichroism (CD).[39] We can apply this characteristic to estimate the degree of molecular ordering in the nonaqueous, chiral bilayer.

Absorption maxima of **6** (Phe-Ole) and **7** (Azo-Ole) in chlorocyclohexane are located at 255 and 355 nm, respectively, and the phase transition at elevated temperatures does not affect the spectral pattern (data not shown). Figure 3 shows their CD spectra. A chlorocyclohexane dispersion of **7** (Azo-Ole) (0.3 mM) gave $[\theta]_{355} = -3.0 \times 10^5$ deg·cm^2·dmol^{-1} at 1 °C. This value is close to that of the above-mentioned nonhelical aqueous bilayer that possesses the identical chiral unit,[39] although the latter $[\theta]$ value is even more enhanced once the helical superstructure is formed ($[\theta]_{\max} = 1.4 \times 10^6$). It is obvious that the azobenzene moiety in the bilayer of **7** (Azo-Ole) is aligned regularly. The magnitude of $[\theta]_{355}$ was lessened as the temperature rose, and the CD peak almost disappeared at 17 °C (Figure 3a). Upon cooling, the original CD intensity was restored at the respective temperature after 30 min of aging.

A chlorocyclohexane dispersion of **6** (Phe-Ole) (1.0 mM) also displayed a CD intensity of $[\theta]_{270} = +21 \times 10^4$ deg·cm^2·dmol^{-1} at 3 °C (Figure 3b). This value is about two thirds of that ($\pm 33 \times 10^4$ deg·cm^2·dmol^{-1}) of an aqueous bilayer possessing an analogous chromophore structure.[39] The peak intensity at 270 nm decreases with increasing temperature and becomes undetectable at 13 °C. It is recovered in the cooling process but thermal hysteresis was observed (inset of Figure 3b). Apparently it takes longer (ca. 1 h under the conditions in Figure 3) for **6** (Phe-Ole) to regain the bilayer structure from the monomeric state.

The different hysteresis behaviors of bilayers **6** (Phe-Ole) and **7** (Azo-Ole) appears to arise from a change in the stacking energies (van der Waals force) of the phenylene and azobenzene chromophores. Because of the stronger stacking of the azobenzene unit, the component amphiphile can assume the most stable alignment readily in the nonaqueous bilayer of **7** (Azo-Ole). The thermodynamic data in section 8 also confirmed this presumption.

The phase transitions of bilayers might account for the decrease in the CD intensity, as has been established for many aqueous bilayers.[16,39] However, this cannot be the case in the present system, since the decrease starts at temperatures much lower than the beginning of the endothermic peaks in DSC (20 °C for **6** (Phe-Ole) and 27 °C for **7** (Azo-Ole)). Instead, a variation of CMC with temperature seems to cause the CD change. The concentration of **7** (Azo-Ole) used for the CD measurement (3.0×10^{-4} M) happens to be situated between the CMC values at 15 °C (1.7×10^{-4} M) and at 20 °C (3.5×10^{-4} M). Formation and destruction of the bilayer structure with temperature must take place at the concentration used. The same explanation

---

[42] The heat of fusion for the terminal CF_3 group is −22.1 kJ/mol, and that for the CF_2 unit is 5.1 kJ/mol in C_nF_{2n+2} (n = 2–12).[43] Therefore, the energy required to break a hydrogen bond (about 20 kJ/mol) and to melt two perfluorooctyl chains is estimated as 2[(−22.1) + (5.1)7] + 20 = 47.5 kJ/mol.

[43] Starkweather, H. W., Jr. *Macromolecules* **1986**, *19*, 1131–1134.

[44] It was difficult to obtain reliable molecular weight data under the conditions of below 70 °C and above 2 mM because of gel formation and too low vapor pressure, respectively.

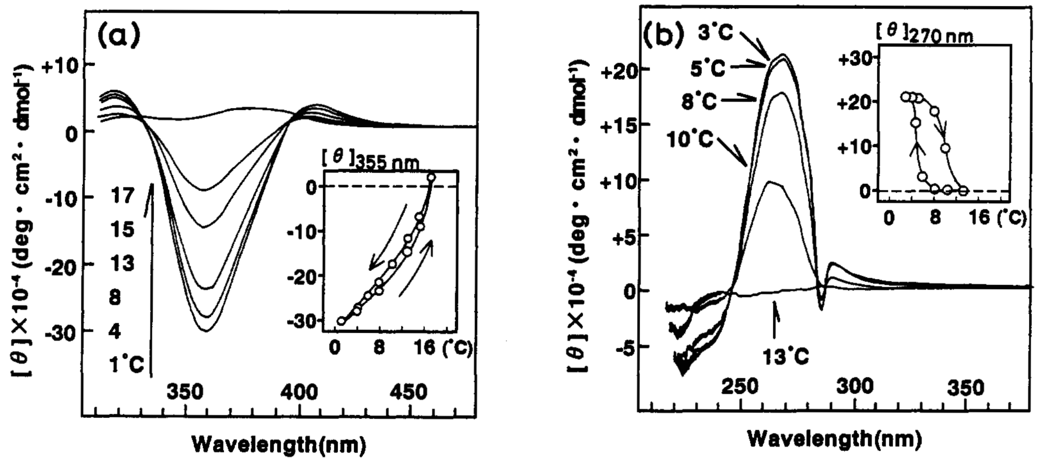

Figure 3. CD spectra of **6** (Phe-Ole) and **7** (Azo-Ole) bilayers in chlorocyclohexane and their thermal hystereses. (a) Bilayer **7** (Azo-Ole) (0.3 mM) in chlorocyclohexane. The inset represents thermal hysteresis of the $[\theta]_{max}$ (355 nm) value. A 30-min interval was kept before the subsequent measurement. (b) Bilayer **6** (Phe-Ole) (1.0 mM) in chlorocyclohexane. The inset shows thermal hysteresis of the $[\theta]_{max}$ (270 nm) value. The interval is the same as in a.

applies to the CD data of the chlorocyclohexane dispersion of **6** (Phe-Ole).

6. Contribution of Hydrogen Bonding to Bilayer Assembly. Contribution of intermolecular hydrogen bonding to the formation of aqueous bilayers has been noticed in many systems.[40,41] The hydrogen bonding should contribute to molecular self-assembly in noncompetitive aprotic media better than in aqueous media. Among the three amphiphiles, bilayers of **3** (Ole) are most convenient for monitoring hydrogen bonding through IR spectroscopy, since their carbonyl stretching vibration bands around 1500 and 3750 cm^{-1} are not interfered with by the bands of the azobenzene or phenylene rings.

In chloroform, where bilayer formation is not probable (see Table 1), the ν_{NH}, $\nu_{C=O}$(amide I), and δ_{NH}(amide II) peaks for **3** (Ole) (20 mM) are located at 3430, 1675, and 1505 cm^{-1}, respectively, indicating the absence of hydrogen bonding.[45] Figure 4 represents FT-IR spectra of **3** (Ole) (20 mM) in chlorocyclohexane at two temperatures: below and close to the phase transition. While this temperature difference affected little the $\nu_{C=O}$(ester) band at 1743 ± 5 cm^{-1}, the ν_{NH} (amides I and II) bands showed temperature dependence. At 15 °C, ν_{NH} (amides I and II) bands appear as singlet peaks at 3312, 1644, and 1536 cm^{-1}, respectively. These wavenumbers are shifted from those of the monomeric amide in chloroform by as much as −118, −31, and +33 cm^{-1}, respectively, and suggest the formation of the hydrogen bond in the "trans" mode.[40,45] At 40 °C where the phase transition starts, the amide peaks are shifted to the same positions as those in chloroform but several percent of the original peaks still remain. The original peak would disappear completely if the dispersion could be heated to higher temperatures. Combined with the molecular weight data at 70 °C (see section 4), these IR data endorse the "bilayer–monomer" phase transition.[46]

7. Conformational Change of the Helical Perfluorooctyl Group. Poly(tetrafluoroethylene) is known to possess helical conformations along the main chain because of the van der Waals repulsions among the fluorine atoms.[47,48] Such a helical structure has been confirmed also in Langmuir Blodgett multilayers of polymers with perfluorooctyl side chains[49] and in vapor-deposited films of *n*-perfluoroalkanes.[50] Its helical pitch, viz. the phase angle of

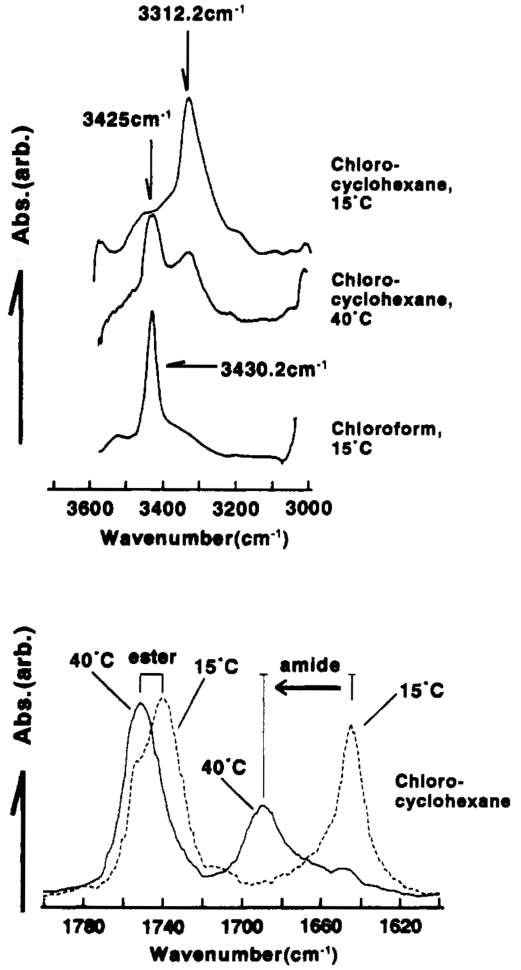

Figure 4. Influence of temperature on the amide and ester bands in FT-IR absorption spectroscopy: **3** (Ole) in chlorocyclohexane (20 mM, the same concentration as in the DSC measurement).

F–C–F's, is affected by temperature and is reflected in the $-CF_2-$ vibrations, as verified by theoretical calculations.[48,50–52]

Figure 5 shows FT-IR spectra of a chlorocyclohexane dispersion of **3** (Ole) (20 mM) in the range 1250–1100 cm^{-1}. Three kinds

---

(45) Nakanishi, N.; Solomon, P. H.; Furutachi, N. *Infrared Absorption Spectroscopy*; Nankodo: Japan, 1989.

(46) The amide band of **7** (Azo-Ole) in chlorocyclohexane also indicated the presence of the hydrogen bonding at 15 °C, that is, below the phase transition temperature.

(47) Bunn, C. W.; Howells, E. R. *Nature* **1954**, *174*, 549–551.

(48) Rabolt, J. F.; Fanconi, B. *Macromolecules* **1978**, *11*, 740–745.

(49) Schneider, J.; Erdelen, C.; Ringsdorf, H.; Rabolt, J. F. *Macromolecules* **1989**, *22*, 3475–3480.

(50) Hsu, S. L.; Reynolds, N.; Bohan, S. P.; Strauss, H. L.; Snyder, R. G. *Macromolecules* **1990**, *23*, 4565–4575.

(51) Zerbi, G.; Sacchi, M. *Macromolecules* **1973**, *6*, 692–699.

(52) Hannon, M. J.; Boerio, F. J.; Koenig, J. L. *J. Chem. Phys.* **1969**, *50*, 2829–2836.

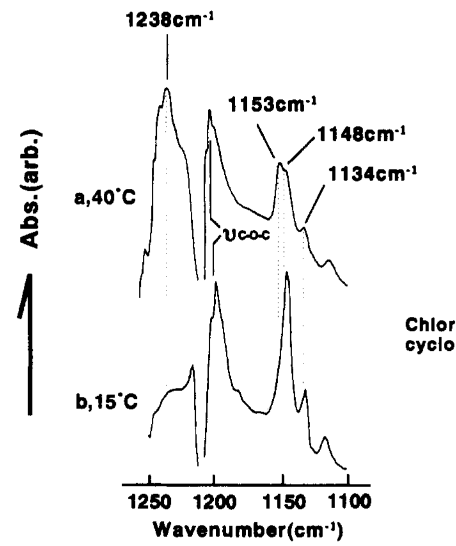

Figure 5. Temperature dependence of the C–F vibrational bands. The sample is the same as in Figure 4.

Table 2. C–F Vibration Bands of **3** (ole) (20 mM) in the Range 1250–1100 cm^{-1}

assignments	$\nu_{as}(CF_2)$, rocking CF_2	$\nu_s(CF_2) + \delta CF_2$		
helical mode[a]	15/7	15/7	13/6	10/3
observed peak (cm^{-1})	1238	1153	1148	1134
relative absorbance[d]				
in $CHCl_3$ 30 °C	*b*	2.2	1.8 (S)[c]	1.1
in chlorocyclohexane 40 °C	3.3	2.1	1.7 (S)	1.1
15 °C	1.7 (S)	none	4.0	1.7

[a] *m*/*n* indicates *m* π turns per *n* carbons, belongs in the D(*m* π/*n*) group. [b] Unreliable due to overscaled peak intensity. [c] Shoulder peak. [d] Defined against the $\nu_{C=O}$ (ester) peak at 1742 cm^{-1}.

of peaks are found at 40 °C: (a) $\nu_s(CF_2)$ at 1134 (s), 1148 (vs), and 1152 (vs) cm^{-1}; (b) $\nu_{as}(CF_2)$ at 1238 (vs) cm^{-1} with shoulders at 1242 (vs) and 1250 (s) cm^{-1}; and (c) ν(C–O–C) at 1203 (vs) and 1226 (shoulder) cm^{-1}. According to theoretical studies,[49–51] we can assign the $\nu(CF_2)$ peaks to the helical chains of varied pitches as given in Table 2. These wavenumbers agree with those observed in chloroform, where no bilayer exists. Cooling to 15 °C in chlorocyclohexane gave rise to large changes in the relative intensities of these signals. The relative intensity was calculated by using the ester peak (1742 cm^{-1}) as an internal standard, since it is not sensitive to temperature change. The IR absorbance at 1152 cm^{-1} (15/7 helix = 7 turns by 15 carbons) decreases, and those at 1148 cm^{-1} (13/6 helix) and 1134 cm^{-1} (10/3 helix) markedly increase upon cooling to 15 °C. The peak at 1238 cm^{-1} (15/7 helix) is weakened concurrently to become a shoulder of the ν(C–O–C) peak at 1221 cm^{-1}. These spectral changes are reversible.

The helical conformation, the angle F–C–F, is loosened to the trans zigzag conformation in the order of 10/3, 13/6, 15/7 helices. Thus, the cooling process leads to increases in tighter helical conformations: a decrease in the 15/7 helix and increases in the 13/6 and 10/3 helices. These intramolecular conformational changes are related to changes in the intermolecular association including the bilayer–monomer phase transition.

8. Thermodynamics of the Self-Assembly Process. In order to understand the above-mentioned, unique self-assembling process, we made a careful thermodynamic examination. It is possible to determine the thermodynamic parameters of self-assembling by measuring surface tension as a function of temperature. We employed two different sets of equations for this purpose. One is based on the Motomura's theory[53,54] and determines entropy changes from the temperature dependence of surface tension γ.

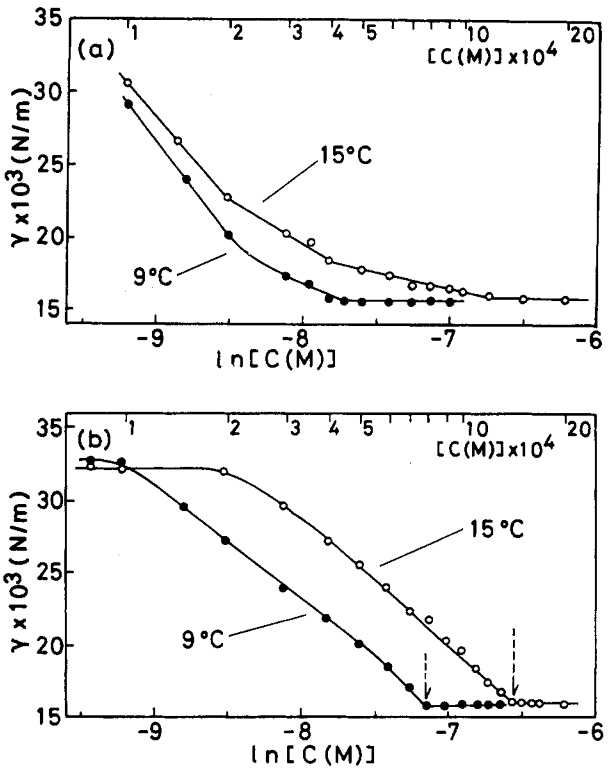

Figure 6. Surface tension of chlorocyclohexane upon addition of **3** (Ole) and **6** (Phe-Ole) under the atmospheric pressure.

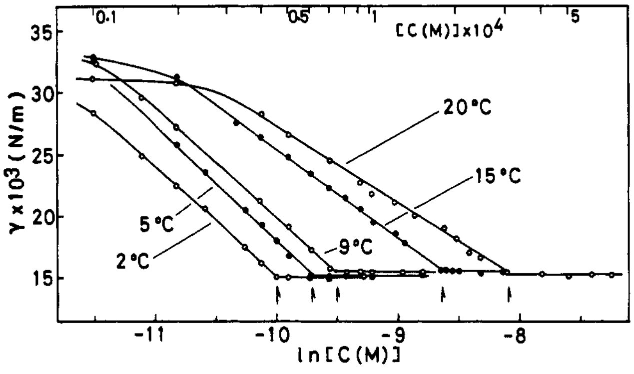

Figure 7. Surface tension of chlorocyclohexane upon addition of **7** (Azo-Ole) under atmospheric pressure.

The second method,[1–3,55,56] as adopted also by Shinoda and others, uses the temperature dependency of CMC values. Neither of these methods assumes a standard state.

(a) Surface adsorption behavior. Figures 6 and 7 show influences of **3** (Ole), **6** (Phe-Ole), and **7** (Azo-Ole) on the surface tension of chlorocyclohexane. All the measurements were performed below phase transition temperatures of dispersed bilayers. The surface tension decreased with increasing amphiphile concentrations from 33 ± 1 mN/m (the value of the pure solvent) to around 15 mN/m. All the γ versus ln[*C* (M)] curves shifted toward the direction of high concentrations through elevation of temperature. The values of surface tension at high concentrations beyond the break point did not depend on temperature and yielded the identical value of 15 mN/m.

---

(53) Motomura, K. *J. Colloid Interface Sci.* **1978**, *64*, 348–355. Motomura, K.; Kajiwara, I.; Ikeda, N.; Aratono, M. *J. Colloid Interface Sci.* **1989**, *38*, 61–69. Matsuguchi, M.; Aratono, M.; Motomura, K. *Bull. Chem. Soc. Jpn.* **1990**, *63*, 17–20 and references cited therein.

(54) Aratono, M.; Okamoto, T.; Motomura, K. *Bull. Chem. Soc. Jpn.* **1987**, *60*, 2361–2365.

(55) Shinoda, K. *J. Phys Chem.* **1977**, *81*, 1300–1302.

(56) Shinoda, K.; Kobayashi, M.; Yamaguchi, N. *J. Phys Chem.* **1987**, *91*, 5292–5294.

Table 3. Adsorption Characteristics of **6** (Phe-Ole) and **7** (Azo-Ole) at the Air/Chlorocyclohexane Interface

amphiphile[a]	T (°C)	Γ_{max} (μmol/m^2)	A_{min} (Å^2/molecule)	CMC × 10^4 (mol/L)	X_{CMC} × 10^5
6 (Phe-Ole)	9	4.0	42	8.1	95
	15	3.8	44	14.0	165
7 (Azo-Ole)	2	3.9	43	0.45	0.53
	5	3.7	45	0.61	0.72
	9	3.5	48	0.77	0.91
	15	3.0	55	1.70	2.02
	20	2.4	69	3.50	4.15
$C_8F_{17}C_{12}H_{25}$[32]	30			2400	

[a] It is difficult to determine the values for **3** (Ole), see section 8.

Common fluorocarbon surfactants reduce the surface tension of water from 72 to 15 mN/m.[17,57] It is obvious, therefore, that the present amphiphiles display surface activities comparable to those of aqueous amphiphiles.

Assuming that monomeric amphiphiles are adsorbed at the air/chlorocyclohexane interface to form a monolayer, we can determine the amount of absorbed amphiphiles at the surface, Γ, and the average occupied area per molecule, A, from the Gibbs adsorption isotherm (eq 1) and eq 2, respectively.[53]

$$\Gamma\ (\mathrm{mol/m^2}) = -(1/RT)[\gamma/\ln(C)]_{\mathrm{P,T}} \qquad (1)$$

$$A = 1/(N_{\mathrm{A}}\Gamma),\quad N_{\mathrm{A}} = \text{Avogadro's number} \qquad (2)$$

It is difficult to pinpoint the break in the curves of **3** (Ole) due to their concave downward shapes (Figure 6a). In contrast, all curves of **6** (Phe-Ole) and **7** (Azo-Ole) in Figures 6b and 7 display slightly upward concave and sharp break points. In order to treat the data in terms of the simplest phase equilibrium, i.e., monomer vs single sort of aggregate, the curve should be straight or upward concave below the break point. Application of eq 1 to the curves of **3** (Ole) is not desirable, since downward concave curves demand the assumption of stepwise adsorption (monomer, dimer, trimer, etc.). This implies that the cooperativity of the assembling process of **3** (Ole) is not sufficient relative to those of **6** (Phe-Ole) and **7** (Azo-Ole). Thus, we avoided thermodynamic analysis of adsorption of **3** (Ole). As opposed to the chlorocyclohexane dispersion of **3** (Ole), its methylcyclohexane dispersion gave slightly upward curves similar to those in Figure 7.[34] The use of a less polar solvent appears to produce better self-assembly in return for a risk of crystallization. A similar solvent effect on the process of amphiphilic assembly was reported also for semi-fluorinated alkanes.[30,32]

The Γ values of **6** (Phe-Ole) and **7** (Azo-Ole) were enhanced with increasing amphiphile concentrations and saturated at their break points at all the temperatures used (data not shown). As mentioned below, the maximum A values at the break point are almost the same as the cross sectional areas of **6** (Phe-Ole) and **7** (Azo-Ole), so the break point must be the critical point for adsorption from either monomer or bilayer phases and is equivalent to the CMC.

(b) Molecular Area of the Adsorbed Monolayer. Table 3 summarizes the maximum Γ values and minimum A values obtained at the CMC's. Related ammonium amphiphile, **1**, that possesses double fluorocarbon chains similar to **6** (Phe-Ole) and **7** (Azo-Ole), provides stable, insoluble monolayers at the air/water interface. Its molecular area at the collapse pressure is 47 ± 3 Å^2/molecule, and extrapolation of the condensed π-A region intersects the axis of the molecular area at 59 ± 2 Å^2/molecule.[20,58] As shown in Table 3, the A_{min} value of the adsorbed monolayer of **7** (Azo-Ole) ranges from 43 to 69 Å^2/molecule. There is good correspondence between the molecular area of insoluble monolayer **1** and that of the adsorbed monolayer **7** (Azo-Ole). The A_{min} value increases with elevating temperature. This tendency corresponds to expansion of the insoluble monolayer of **1** with temperature. The absorbed monolayer of **6** (Phe-Ole) behaves similarly.

In general, adsorbed monolayers of aqueous single-chained surfactants display minimum molecular areas several times the cross sectional area of the amphiphile: $C_8F_{17}COOLi$, 88.7 Å^2/molecule at 25 °C;[59] $C_{12}H_{25}N(CH_3)_3Cl$, 67 Å^2/molecule at 15 °C;[54] $C_{12}H_{25}(OC_2H_4)_8OH$, 66 Å^2/molecule at 25 °C;[60] $C_{12}H_{25}SO_3Na$, 56 Å^2/molecule at 25 °C.[61] Unlike these loose molecular packings, **6** (Phe-Ole) and **7** (Azo-Ole) form densely packed, adsorbed monolayers due to their superior self-assembling properties.

(c) CMC Value. The critical membrane (micelle) concentration (CMC) represents the saturation solubility of monomeric species and is used as a key criterion for the stability of molecular assemblies without regard for the nature of the amphiphiles.[62] When saturation solubilities among different solvent systems are compared, it is preferable to use the molar fraction, X, in place of the conventional molar concentration (mol/L). Table 3 includes conventional CMC values and the molar fraction at CMC, X_{CMC}. The X_{CMC} values of **6** (Phe-Ole) and **7** (Azo-Ole) dispersed in chlorocyclohexane are in the range 10^{-6}–10^{-5}. These values are larger than those of aqueous bilayers (below 10^{-7})[63] but smaller than those of aqueous micelles[54,57,60,61] and nonaqueous micelles of the semi-fluorocarbons (above 10^{-4}).[32] The aggregation stability of the present nonaqueous bilayers, therefore, is placed between those of micelles and aqueous bilayers.

(d) Thermodynamic Quantities of Surface Adsorption and Bilayer Formation. According to the Motomura's method,[53,54] we can estimate from eqs 3 and 4 entropy changes associated with adsorption of amphiphiles from the monomeric and bilayer states. The entropy change of the monomer/bilayer process at CMC is obtained from eq 5. These thermodynamic quantities are obtained under the conditions of CMC and atmospheric pressure and do not refer to the standard state. The three phases of monomer, bilayer, and adsorbed monolayer are in equilibrium at CMC (ΔG = 0). Equation 6, therefore, can be used for computing ΔH.

$$\Delta S_{\mathrm{M}}^{\mathrm{Ad}}\ [\mathrm{J/(K{\cdot}m^2)}] = S(\text{adsorbed}) - S(\text{monomer}) = -(\delta\gamma/\delta T)_{\mathrm{p,C}},\quad \text{at } C < \mathrm{CMC} \qquad (3)$$

$$\Delta S_{\mathrm{B}}^{\mathrm{Ad}}\ [\mathrm{J/(K{\cdot}m^2)}] = S(\text{adsorbed}) - S(\text{bilayer}) = -(\delta\gamma/\delta T)_{\mathrm{p,C}},\quad \text{at } C \geq \mathrm{CMC} \qquad (4)$$

$$\Delta S_{\mathrm{M}}^{\mathrm{B}}\ [\mathrm{J/(K{\cdot}mol)}] = S(\text{bilayer}) - S(\text{monomer}) = [\Delta S_{\mathrm{M}}^{\mathrm{Ad}} - \Delta S_{\mathrm{B}}^{\mathrm{Ad}}]/\Gamma_{\max} \qquad (5)$$

$$\Delta H_{\mathrm{M}}^{\mathrm{B}}\ [\mathrm{J/(mol)}] = H(\text{bilayer}) - H(\text{monomer}) = T\Delta S_{\mathrm{M}}^{\mathrm{B}} \qquad (6)$$

We began with the data of amphiphile **7** (Azo-Ole) (Figure 7), since it gave the smallest CMC value among the three

---

(57) Caporiccio, G.; Burzio, F.; Carniselli, G.; Biancardi, V. *J. Colloid Interface Sci.* **1984**, *98*, 202–209. Kunieda, H.; Shinoda, K. *J. Phys Chem.* **1976**, *80*, 2468–2470. Shinoda, K.; Hato, M.; Hayashi, T. *J. Phys Chem.* **1972**, *76*, 909–914.

(58) Higashi, N.; Kunitake, T. *Chem. Lett.* **1986**, 105–108. Claesson, P. M.; Herder, P. C.; Berg, J. M.; Christenson, H. K. *J. Colloid Interface Sci* **1990**, *136*, 541–551.

(59) Mesa, C. L.; Sesta, B. *J. Phys Chem.* **1987**, *91*, 1450–1454.

(60) Rosen, M. J.; Cohen, A. W.; Dahanayake, M. *J. Phys Chem.* **1982**, *86*, 541–545.

(61) Dahanayake, M.; Cohen, A. W.; Rosen, M. J. *J. Phys Chem.* **1986**, *90*, 2413–2418.

(62) The aggregation phenomena of conventional surfactants and bilayer-forming compounds can be discussed by the same measure (CMC value), although their aggregation properties are clearly distinguishable (see section 10).

(63) Kunitake, T.; Okahata, Y.; Shimomura, M.; Yasunami, S.; Takarabe, K. *J. Am. Chem. Soc.* **1981**, *103*, 5401–5413. Okahata, Y.; Tanamachi, S.; Nagai, M.; Kunitake, T. *J. Colloid Interface Sci.* **1981**, *82*, 401–417.

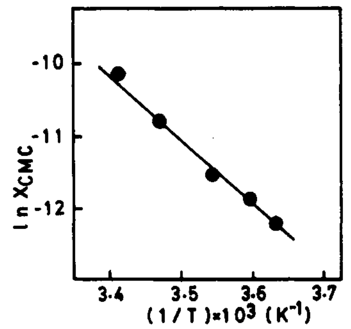

Figure 8. Temperature dependences of the critical membrane concentrations of **3** (Ole), **6** (Phe-Ole), and **7** (Azo-Ole) in chlorocyclohexane.

amphiphiles. The γ versus T plots at the CMC or the temperature range of 2–20 °C gave a linear relation (data not shown) with a slope, $\Delta S_{\mathrm{M}}^{\mathrm{Ad}}$, of –0.70 ± 0.05 mJ/(K·m²). The γ values above the CMC are 15.2 mN/m and are little affected by temperature. This means that the $\Delta S_{\mathrm{B}}^{\mathrm{Ad}}$ is virtually zero. Substitution of these ΔS values and $\Gamma_{\max}$ of Table 3 into eq 5 gives the $\Delta S_{\mathrm{M}}^{\mathrm{B}}$ value of –210 ± 20 J/(K·mol) in this temperature range. In fact, $\Delta S_{\mathrm{M}}^{\mathrm{B}}$ increases slightly with temperature, but the change is within experimental error. The corresponding $\Delta H_{\mathrm{M}}^{\mathrm{B}}$ value is estimated from eq 6 to be –60 ± 6 kJ/mol.

The same thermodynamic quantities are also evaluated by using general eqs 7 and 8. As given in Figure 8, a linear relation was observed between $\ln(X_{\mathrm{CMC}})$ and $1/T$. The $\Delta H_{\mathrm{M}}^{\mathrm{B}}$ and $\Delta S_{\mathrm{M}}^{\mathrm{B}}$ values

$$\Delta H_{\mathrm{M}}^{\mathrm{B}}\ [\mathrm{J/mol}] = H(\text{bilayer}) - H(\text{monomer}) = R[\delta \ln(X_{\mathrm{CMC}})/\delta(1/T)]_{\mathrm{p}} \quad (7)$$

$$\Delta S_{\mathrm{M}}^{\mathrm{B}}\ [\mathrm{J/(K{\cdot}mol)}] = S(\text{bilayer}) - S(\text{monomer}) = \Delta H_{\mathrm{M}}^{\mathrm{B}}/T \quad (8)$$

were thus determined to be –69 ± 5 kJ/mol and –230 ± 20 J/(K·mol), respectively. These values agree with those calculated from eqs 3–6 within experimental error. Moreover, the enthalpy change as determined from the surface tension measurement for bilayer formation (–70 kJ/mol) does agree with the endothermic change in the DSC thermogram (+69 kJ/mol) for bilayer disintegration. We can again confirm that the endothermic process in DSC corresponds to the bilayer-to-monomer transition.

The thermodynamic relations among monomer, surface monolayer, and dispersed bilayer of **7** (Azo-Ole) are summarized in Figure 9. These thermodynamic quantities illustrate important features of the aggregation process. First of all, the $\Delta H_{\mathrm{M}}^{\mathrm{B}}$ and $\Delta S_{\mathrm{M}}^{\mathrm{B}}$ terms for the molecular association in solvent assume large, negative values. This indicates that the enthalpic force governs the formation of the nonaqueous bilayer. This is a thermodynamic situation similar to the hydrophobic force in water[55,56,64] and the solvophobic force in water-like organic media.[1–3,7] The cratic and unitary entropy[65] components (–90 and –140 J/(K·mol), respectively) are negative, and their magnitudes are larger than those of an aqueous fluorocarbon micelle.[66] The greater (negative) unitary ΔS of the bilayer implies that their component molecules should be aligned much more regularly than those in the aqueous micelle. The difference in the cratic ΔS term can be explained by considering larger aggregation numbers relative to those of the aqueous micelle. Secondly, there are no detectable changes in the thermodynamic values for the conversion between the surface monolayer and dispersed bilayer. The two organized states, therefore, are thermodynamically identical, and they must possess analogous structural characteristics. Thirdly, the entropy change in the monomer-to-monolayer conversion is negatively 14 times greater than that of adsorption of dodecylammonium ion at the air/water interface.[53,54] The present fluorocarbon "amphiphile", therefore, produces a much more ordered monolayer than the micellar surfactant (dodecylammonium ion). This fact is related to the above feature.

9. Contribution of Aromatic Stacking and Hydrogen Bonding to Self-Assembly. The CMC values of **7** (Azo-Ole) are 1–2 orders of magnitude smaller than those of **6** (Phe-Ole). This is a reflection of the greater stabilization effect of the azobenzene unit relative to the benzene unit in the particular solvent. This effect also causes the difference in the thermal hysteresis on their CD spectra (see section 5). As mentioned above, the nonchromophoric **3** (Ole) displays inferior cooperativity of association to those of the chromophoric amphiphiles, although the identical adsorption behavior, the same γ (ca. 15 mN/m) and the temperature dependence, is found at higher concentrations. The thermodynamic stability, therefore, is given in the following order: **7** (Azo-Ole)) > **6** (Phe-Ole) ≫ **3**(Ole). It is clear that van der Waals attractive forces among the aromatic units enhance the aggregate stability, although their contribution to the total enthalpic change cannot be estimated readily.

The intermolecular hydrogen bonding among the amide unit of the connector module similarly promotes efficient assembling (see section 6). If we assume that breaking of a hydrogen bond in the dissociation process requires the widely quoted H-bond energy (approximately 20 kJ/mol), the contribution of ΔH(H-bond) to the total enthalpy change amounts to roughly 30% for **7** (Azo-Ole), 30% for **6** (Ph-Ole) and 50% for **3** (Ole) (from the DSC data).

From the foregoing results we can conclude that the bilayer formation is enthalpy driven. The enthalpic association force[65] is divided into the following three factors: (1) immiscibility (solvophobic force) of double fluorocarbon (FC) chains against aprotic hydrocarbon (HC) media (FC-Chain/HC-Medium), (2) intermolecular hydrogen bonding (H-bond), and (3) van der Waals forces among the aromatic rings (stacking). Unlike the aqueous system, we need not take into account the effect of "solvent structuring" such as the iceberg formation. The overall enthalpy change, therefore, can be expressed by

$$\Delta H_{\mathrm{M}}^{\mathrm{B}} = \Delta H(\text{FC-Chain/HC-Medium}) + \Delta H(\text{H-bond}) + \Delta H(\text{stacking}) \quad (9)$$

10. Nature of Solvophobic Force. Before discussing the solvophobic force, let us begin with the origin of the hydrophobic force. The major driving force of amphiphile aggregation in water had been considered for a long time to be the hydrophobic effect that is entropy driven as related to the water structuring.[66] During the late 1970s[55] and 1980s,[1–3,56,63] however, it was pointed out that water structuring was not responsible for aggregation of amphiphilic molecules. Water structuring itself should promote hydration of alkyl chains of amphiphiles and disintegrate aggregates. The solute aggregation is instead produced by the differences between the cohesive energies of medium (water) molecules and of alkyl chains. The "hydrophobic force" observed in highly structured water is thus rooted in the same thermodynamic origin as solvophobic forces observed for molecular association in less-structured protic media such as hydrazine[1–3] and formamide.[7] Formation of extensive hydrogen-bonding networks of medium is not relevant to assembly of the amphiphile. The thermodynamic data presented in this paper clearly establish that the same situation exists in aprotic media which totally lack in the hydrogen-bonding capability. The molecular assembly in

---

(64) Silveston, R.; Kronberg, B. *J. Phys Chem.* **1989**, *93*, 6241–6246.

(65) The entropy change may be correspondingly expressed as $\Delta S_{\mathrm{M}}^{\mathrm{B}} = R[\ln(X_{cmc})] + \Delta S(\text{F-Chain/H-Medium}) + \Delta S(\text{H-bond}) + \Delta S(\text{stacking}) = \mathrm{R}[\ln(X_{cmc})] + \Delta S(\text{unitary term})$, where $R[\ln(X_{cmc})]$ is the cratic entropy arising from a decrease in chemical species.

(66) For micelle formation of lithium perfluorooctanesulfonates in water, the cratic entropy changes were reported to be –73.8 (30.5 °C) to –57.4 (165 °C) J/(K·mol), and the unitary entropy change was a constant value of –54.5 J/(K·mol) in this temperature range.[56]

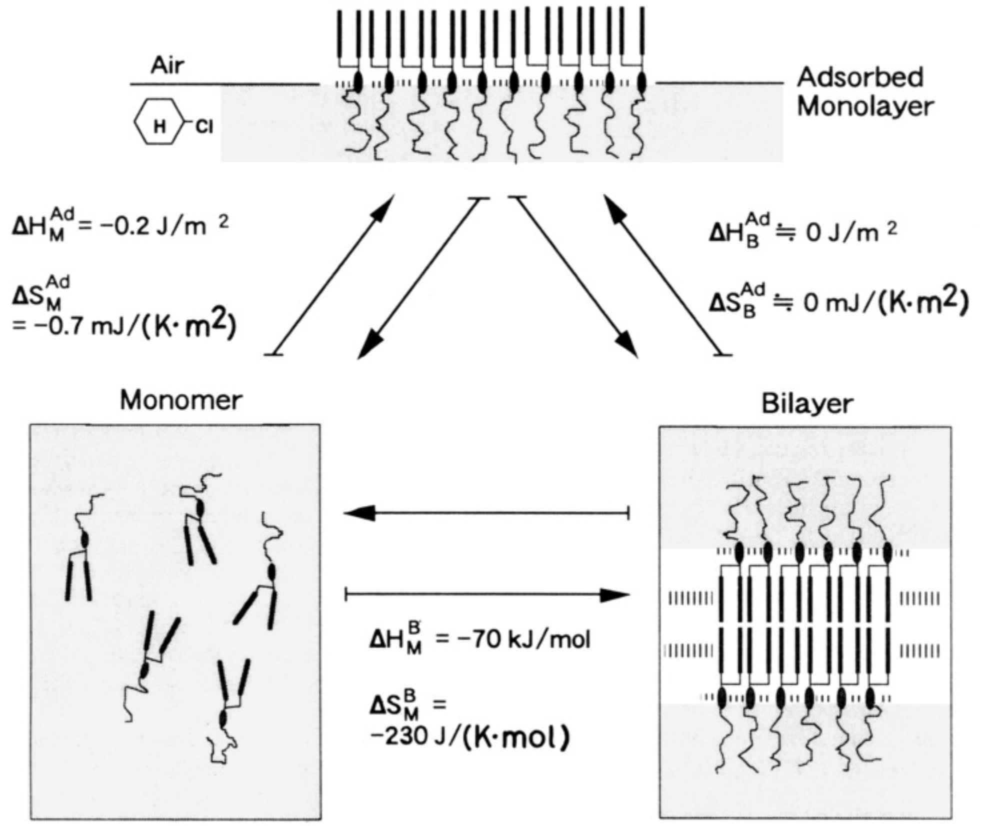

Figure 9. Thermodynamic relations of surface adsorption and bilayer formation of the fluorocarbon/hydrocarbon amphiphilie **7** (Azo-Ole).

these cases is commonly derived from immiscibilities of solutes against solvents (i.e., cohesive energy differences), regardless of the hydrogen-bonding ability of solvents.

The cohesive energy, intermolecular force, of a liquid can be considered in terms of surface tension. The surface tension of liquids decreases in the following order: water (72 mN/m) > water-like media (60–70 mN/m) ≫ hydrocarbons (around 30 mN/m) > perfluorocarbons (10–15 mN/m). The first three assembling systems (in water, in water-like media, and in aprotic hydrocarbon media) possess the *common characteristic that the cohesive force of medium molecules is stronger than that of solute molecules (fluorocarbon or hydrocarbon chains)*. It is not going too far to say that the solute chains are forced to be removed away from tighter aggregates of medium molecules, resulting in molecular assemblies. The active role in the assembling process lies in the medium rather than in the alkyl chains. In this sense, the present fluorocarbon bilayer can be perceived as showing "*passive*" solvophobicity because of the weaker cohesive forces of solutes.

The magnitude of the solvophobicity is related to the interfacial tension of a given liquid combination. The interfacial tensions of water/perfluoroalkanes (50–60 mN/m) and of water/hydrocarbons (ca. 45 mN/m) as estimated from surface tensions are 3–6 times as large as those of hydrocarbons/perfluoroalkanes (10–15 mN/m). This means that the solvophobicity of fluorocarbon assemblies in aprotic hydrocarbon media is less pronounced than that of aqueous aggregates. The weaker solvophobicity may be supplemented by other attractive forces. The stacking and H-bond terms act as additional attractive forces in the present system and lead to improved bilayer stability.[67] The enthalpy change of the monomer-to-bilayer conversion of **7** (Azo-Ole) in chlorocyclohexane (–70 kJ/mol) is close to the corresponding value of an aqueous fluorocarbon micelle (lithium perfluorooctanesulfonate, –72.9 kJ/mol).[56,68] The thermodynamic stabilization of the present bilayers reaches that of the aqueous micelle, but it does not exceed that of the aqueous bilayer.[69] The present bilayer disintegrates into monomers at high temperature, while aqueous bilayers maintain their aggregate structure even above the phase transition temperature. It is natural, therefore, that the semi-fluorinated alkanes for which additional aggregation forces are not operative yield less stable (CMC, ca. 200 mM)[32] aggregates in organic media even at room temperature.

The preceding solvophilic/solvophobic relationship may be reversed. We have reported formation of bilayer assemblies in an aprotic fluorocarbon medium.[71] In this case, amphiphilic molecules, such as **9**, are composed of double hydrocarbon chains

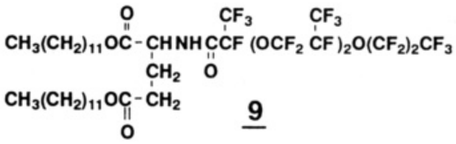

$$\begin{array}{l} CH_3(CH_2)_{11}O\overset{\displaystyle O}{\overset{\|}{C}}\text{-}CHNH\underset{\underset{\displaystyle O}{\|}}{C}\overset{\displaystyle CF_3}{\overset{|}{C}}F\,(OCF_2\overset{\displaystyle CF_3}{\overset{|}{C}}F)_2O(CF_2)_2CF_3 \\ \qquad\qquad\qquad\quad CH_2 \\ CH_3(CH_2)_{11}O\underset{\underset{\displaystyle O}{\|}}{C}\text{-}CH_2 \end{array}$$

9

as the solvophobic moiety and flexible perfluoroalkyl chains as the solvophilic moiety. These particular compounds possess "reversed" amphiphilicity relative to that described in this paper.

It is known that the free energy change for adsorption of perfluoroalkyl surfactants at the perfluorohexane/water interface is 290 J/mol (per $-CF_2-$, 25 °C) larger than that at the hexane/water interface. On the contrary, the free energy change for the adsorption of hydrocarbon surfactants at the hexane/water interface is 550 J/mol (per $-CH_2-$) larger than that at the

---

(67) Frank, H. S.; Evans, M. W. *J. Chem. Phys.* **1945**, *13*, 507–532. Nemethy, G.; Scheraga, H. A. *J. Chem. Phys.* **1962**, *36*, 3401–3417.

(68) We have observed aprotic bilayer formation from double-chained fluorocarbon "amphiphiles" which possess neither aromatic stacking nor hydrogen-bonding capabilities by selecting less polar ethylcyclohexane as the solvent (unpublished results in these laboratories).

(69) This value does not include the Coulombic term and is not affected by temperature in the range from 30.5 to 165 °C.

(70) Unfortunately, there are no thermodynamic data available for the formation of aqueous fluorocarbon bilayers. The difference in stability between aqueous bilayers and the present aprotic bilayers can be inferred from CMC data (see section 8c).

(71) Kuwahara, H.; Hamada, M.; Ishikawa, Y.; Kunitake, T. *J. Am. Chem. Soc.* **1993**, *115*, 3002–3003.

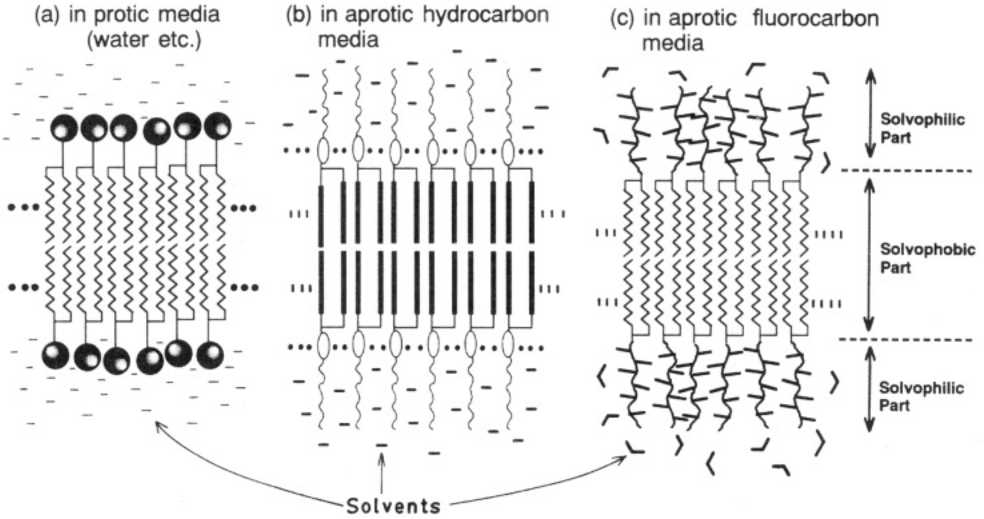

Figure 10. Generalized bilayer concept. (a and b) The cohesive force of medium molecules is *stronger* than that of solute alkyl chains. (c) The force of medium molecules is *weaker* than that of solute alkyl chains.

perfluorohexane/water interface.[72] The latter value is nearly two times as large as the former. Thus, assembly of hydrocarbon chains in fluorocarbon media must be more favorable than assembly of fluorocarbon chains in hydrocarbon media at least in the thermodynamic point of view.

11. Conclusion. These results establish that assembly of molecular bilayers is a widely observable phenomenon. *Organized molecular assemblies are produced in any medium if the "amphiphilic/amphiphobic" nature of the solute molecules is properly designed.* Figure 10 represents the generalized bilayer concept. Self-assembling bilayers can be formed in protic media, in aprotic hydrocarbon media, or in aprotic fluorocarbon media. The common driving force of the molecular assembly is the solute/solvent immiscibilities (enthalpic force) that arise from differences in cohesive energy between the solute (amphiphile) and solvent. The cohesive energy of the solvent is greater than that of the solute in the cases of a and b, but this relation is reversed in c. Therefore, the magnitude of the cohesive energy of the solute *per se* is not relevant for promoting effective molecular assembly. Further expansion of the generalized concept is possible by employing appropriate solute/solvent combinations. The concept should become a powerful, strategic instrument to open up new possibilities for a broad area of supramolecular chemistry.

Experimental Section

Synthesis. *p*-Toluenesulfonate Salt of *O,O'*-Bis(1*H*,1*H'*,2*H*,2*H'*-perfluorodecyl)-L-glutamate (10). 1*H*,1*H'*,2*H*,2*H'*-perfluorodecan-1-ol (13.0 g, 28 mmol), L-glutamic acid (1.47 g, 10 mmol), and *p*-toluenesulfonic acid monohydrate (3.0 g, 15.8 mmol) were suspended in 100 mL of toluene and heated to reflux for 10 h with a Dean Stark trap. The suspension turned homogeneous. White precipitates were collected at room temperature and were recrystallized twice from ethanol: yield 9.5 g (78%); colorless powder, mp 115 → 130 °C (arrow indicates the liquid crystalline region); IR (KBr) ν(C═O) 1750 cm^{-1}, ν(C—F) 1150–1210 cm^{-1}.

***p*-Toluenesulfonate Salt of *O,O'*-Bis(1*H*,1*H'*,2*H*,2*H'*-perfluorododecyl)-L-glutamate (11).** The same procedure as used for **10** was employed. Recrystallization (twice) from methanol/ethanol (1/1, v/v) gave colorless powders of **11** in 68% yield, mp 125 → 156 °C; IR (KBr) ν(C═O) 1750 cm^{-1}, ν(C—F) 1150–1210 cm^{-1}.

***N*-(*Z*)-(9-Octadecen-1-oyl)-*O,O'*-bis(1*H*,1*H'*,2*H*,2*H'*-perfluorodecyl)-L-glutamate (3).** (*Z*)-9-Octadecenoyl chloride (1.5 g, 4.8 mmol) was added dropwise at room temperature into a stirred solution of **10** (2.0 g, 1.6 mmol) and triethylamine (0.66 g, 6.5 mmol) in 40 mL of dry 1,1,2-trifluoro-1,2,2-chloroethane, and the reaction mixture was stirred at about 30 °C for 120 h. The mixture was washed with saturated aqueous NaCl (200 mL × 3). Evaporation of the dried ($MgSO_4$) organic layer followed by recrystallization of the residue from methanol (3 times) gave 1.3 g (62%) of a white powder: mp 62 °C; TLC (silica gel/$CHCl_3$) R_f 0.6; IR (KBr) ν(N—H) 3320 cm^{-1}, ν(C—H) 2920, 2850 cm^{-1}, ν(C═O, ester) 1740 cm^{-1}, ν(C═O, amide) 1645 cm^{-1}, ν(C—F) 1150–1210 cm^{-1}; ^{1}H-NMR (250 MHz, $CDCl_3$, 30 °C) δ 0.88 (t, 3H, –CH_3), 1.25–1.40 (m, 20H, –CH_2–), 1.60 (m, 4H, β-CH_2– to –CH═CH–), 1.90–2.10 (m, 5H, –CH_2—C═ and –CH– adjacent to the chiral carbon), 2.18–2.25 (m, 3H, NCO—CH_2 and another –CH– adjacent to the chiral carbon), 2.4–2.6 (m, 6H, CF_2—CH_2– and OC(═O)—CH_2–), 4.3–4.5 (m, 4H, –CH_2—O), 4.65 (sextet, 1H, CH—N), 5.34 (m, 2H, CH═CH), 6.09 (d, 1H, NH). Anal. Calcd for $C_{43}H_{47}O_5NF_{34}$: C, 39.61; H, 3.63; N, 1.07. Found: C, 39.74; H, 3.65; N, 1.09.

***N*-(*Z*)-(9-Octadecen-1-oyl)-*O,O'*-bis(1*H*,1*H'*,2*H*,2*H'*-perfluorododecyl)-L- glutamate (4).** This compound was prepared from **11** and (*Z*)-9-octadecenoyl chloride, according to the method used for **3**. Recrystallization from methanol and then from ethanol gave a white powder in yield 31%, mp 107–108 °C: TLC (silica gel/$CHCl_3$) R_f 0.7; IR (KBr) ν(N—H) 3320 cm^{-1}, ν(C—H) 2920, 2850 cm^{-1}, ν(C═O, ester) 1740 cm^{-1}, ν(C═O, amide) 1645 cm^{-1}, ν(C—F) 1150–1210 cm^{-1}; ^{1}H-NMR (400 MHz, $CDCl_3$) δ 0.88 (t, 3H, –CH_3), 1.3–1.6 (m, 24H, –CH_2–), 2.00 (sextet, 4H, —CH_2—C═), 2.22 (t, 2H, NCO—CH_2), 2.45 (m, 6H, C(═O)—CH_2–), 4.45 (m, 4H, –CH_2—OC(═O)), 4.65 (sextet,1H, CH—N), 5.35 (m, 2H, CH═CH), 6.09 (d, 1H, NH). Anal. Calcd for $C_{47}H_{47}O_5NF_{42}$: C, 37.54; H, 3.15; N, 0.93. Found: C, 37.34; H, 3.11; N, 0.95.

(*Z*)-9-Octadecenyl *p*-Toluenesulfonate (12). *p*-Toluenesulfonyl chloride (40 g, 0.2 mol) in 100 mL of toluene was added dropwise over 2 h into an ice-cooled solution of (*Z*)-9-octadecen-1-ol (26.9 g, 0.1 mol), pyridine (50 mL), and toluene (50 mL) with stirring. The reaction mixture was stirred for 4 h at about 0 °C, and then 350 mL of 7 wt % hydrochloric acid was added. The organic layer was washed with water (100 mL × 3) and dried over $MgSO_4$. Solvent removal gave 21.9 g (52%) of **12** as a colorless oil: TLC (silica gel/CHCl3) R_f 0.7; IR (neat) ν(C—H) 2925, 2850 cm^{-1}, phenylene 1600, 1500 cm^{-1}, ν(S═O) 1360, 1185 cm^{-1}.

4-[(*Z*)-9-Octadecenyloxy]benzoic Acid (13). The preceding product **12** (7.0 g, 17 mmol) was added to a hot aqueous solution of *p*-hydroxybenzoic acid (2.8 g, 17 mmol) and KOH (85%, 1.2 g, 1.8 mmol). After the mixture was refluxed for 7 h, aqueous KOH (1.2 g in 20 mL) was added. The reaction mixture refluxed again for 10 h, and the solvent was removed in vacuo. The residues were dissolved in 200 mL of hot water and neutralized with hydrochloric acid to pH 2. White precipitates were collected, dried, and recrystallized from acetonitrile. Extraction of the recrystallized products with hot hexane gave 2.5 g (39%) of **13** as colorless crystals: mp 40 → 110 °C; TLC (silica gel/$CHCl_3$) R_f 0.7; IR (neat) ν(C—H) 2920, 2850 cm^{-1}, ν(C═O, CO_2H) 1680 cm^{-1}, phenylene 1600, 1500 cm^{-1}, ν(C—O—C) 1170 cm^{-1}; ^{1}H-NMR (60 MHz, $CDCl_3$) δ 0.9 (t, 3H, –CH_3), 1.3–1.6 (m, 24H, –CH_2–), 2.0–2.1 (m, 4H, O—CH_2–), 4.0 (t, 2H, —CH_2—C═), 5.3 (t, 2H, CH═CH), 6.85 (d, 2H, aromatic), 8.0 (d, 2H, aromatic).

***N*-[[4-[[(*Z*)-9-Octadecenyl]oxy]phenyl]carbonyl]-*O,O'*-bis-(1*H*,1*H'*,2*H*,2*H'*-perfluorodecyl)-L-glutamate (6).** **13** (0.8 g, 1.9 mmol)

---

[72] Mukerjee, P.; Handa, *J. Phys. Chem.* **1981**, *85*, 2298–2303.

was added to 20 mL of $SOCl_2$ and refluxed for 5 h. Excess $SOCl_2$ was removed in vacuo to give a colorless liquid product. This crude acid chloride was immediately dissolved in 50 mL of dry $CHCl_3$ and added dropwise over 10 min to a stirred solution of **10** (1.5 g, 1.2 mmol) and triethylamine (0.7 g, 6.5 mmol) in 50 mL of $CHCl_3$ and 50 mL of 1,1,2-trifluoro-1,2,2-trichloroethane at room temperature. The mixture was kept stirring for 2 days at room temperature and then washed with saturated aqueous NaCl (200 mL × 3). Solvent removal from the dried ($MgSO_4$) organic layer followed by recrystallization from methanol gave a mixture of two components as a colorless powder (Kieselgel 60 Merck, $CHCl_3$, R_f 0 and 0.7). The powder was purified by column chromatography (5 × 30 cm, Kieselgel 60 GF254 Merck, $CHCl_3$) to give 0.6 g (37%) of **6**(Phe-Ole) as a colorless powder: mp 81 → 92 °C; TLC (silica gel, $CHCl_3$) R_f 0.7; IR (KBr) ν(N—H) 3340 cm^{-1}, ν(C—H) 2920, 2850 cm^{-1}, ν(C=O, ester) 1740 cm^{-1}, ν(C=O, amide) 1640 cm^{-1}, ν(C—O—C) + ν(C—F) 1170–1210 cm^{-1}; ^{1}H-NMR (250 MHz, $CDCl_3$, 30 °C) δ 0.87 (t, 3H, –CH_3), 1.2–1.7 (m, 22H, –CH_2–), 1.82 (m, 2H, β-CH_2– to Ph—O–), 2.02 (m, 4H, —CH_2—C=), 2.14 (sextet, 1H, –CH– adjacent to the chiral carbon), 2.3–2.6 (m, 7H, –CH– adjacent to the chiral carbon, CF_2—CH_2– and OCO—CH_2–), 4.43 (m, 2H, –CH_2—O), 4.49 (octet, 2H, –CH_2—O), 4.80 (sextet, 1H, CH—N), 6.83 (d, 1H, NH), 6.91 and 7.76 (dd, 4H, Ph—H). Anal. Calcd for $C_{50}H_{53}O_6NF_{34}$: C, 42.59; H, 3.79; N, 0.99. Found: C, 42.75; H, 3.93; N, 1.07.

4′-(Ethoxycarbonyl)-1-hydroxyazobenzene (14). Ice-cooled aqueous $NaNO_2$ (12.4 g, 0.18 mol, 100 mL) was cautiously poured into a stirred solution of ethyl *p*-aminobenzoate (25.0 g, 0.15 mol) in hydrochloric acid (35%, 40 g in 300 mL) by keeping the temperature below 5 °C. After 10 min, this mixture which contains the diazonium salt was poured into an ice-cooled aqueous solution of phenol (16.0 g, 0.15 mol) and NaOH (9.2 g, 0.19 mol). The reaction mixture was stirred at about 5 °C for 10 min and neutralized with hydrochloric acid to pH 7. The resulting brown precipitates were collected, washed with water, and dried. The product was extracted with 200 mL of hot isopropyl ether. Solvent removal and recrystallization from toluene gave 37 g (90%) of **14** as a brownish red powder: mp 164 °C; TLC (silica gel, $CHCl_3$) R_f 0.2; IR (KBr) ν(C=O, ester) 1700 cm^{-1}, ν(N=N) 1600 cm^{-1}.

1-Carboxy-4′-[(*Z*)-9-octadecenyl]azobenzene (15). **12** (7.8 g, 18.4 mmol) and **14** (5.0 g, 18.4 mmol) were dissolved in 250 mL of ethanol containing 1.3 g (20 mmol) of 85% KOH and refluxed. The reaction was monitored by TLC of the unreacted sulfonate ester. When the sulfonate ester spot disappeared after 8 h, aqueous KOH (1.3 g, 10 mL) was added to the stirred reaction mixture at room temperature in order to hydrolyze the carboxyl ester group. The mixture was refluxed again for 5 h. Upon cooling to room temperature, the precipitates formed were recrystallized from $CHCl_3$/ethanol (1/5 by volume) to give 5.3 g (59%) of **15** as a reddish yellow powder: mp 144 → 232 °C; TLC (silica gel, $CHCl_3$) R_f 0.2; IR (KBr) ν(O—H) 2660, 2550 cm^{-1}, ν(C=O, COOH) 1690 cm^{-1}, ν(N=N) 1590 cm^{-1}, ν(C—O—C) 1145 cm^{-1}; ^{1}H-NMR (60 MHz, $CDCl_3$) δ 0.9 (t, 3H, –CH_3), 1.3–1.6 (m, 24H, –CH_2–), 2.6 (m, 4H, O—CH_2–), 4.0 (t, 2H, —CH_2—C=), 5.3 (t, 2H, CH=CH), 6.9–8.3 (m, 4H, aromatic).

***N*-[[[[4-[[(*Z*)-9-Octadecenyl]oxy]phenyl]azo]phenyl]carbonyl]-*O*,*O*′-bis(1*H*,1*H*′,2*H*,2*H*′-perfluorodecyl)-L-glutamate (7).** **15** (0.8 g, 1.6 mmol) was mixed with 20 mL of $SOCl_2$ and refluxed for 3 h. Excess $SOCl_2$ was removed in vacuo to give the crude acid chloride (red solid). This was dissolved in 50 mL of $CHCl_3$ and added dropwise to a stirred solution of **10** (2.0 g, 1.6 mmol) and triethylamine (0.7 g, 6.5 mmol) in 50 mL each of $CHCl_3$ and 1,1,2-trifluoro-1,2,2-trichloroethane at room temperature. The reaction mixture was stirred at room temperature for 120 h and was washed with saturated aqueous NaCl (200 mL × 3). The organic layer was dried over $MgSO_4$, and the solid residue was recrystallized three times from methanol to give a mixture of two components as a yellow powder (Kieselgel 60 Merck, $CHCl_3$, R_f 0.2 and 0.5). The product was purified by column chromatography (5 × 30 cm, Kieselgel 60 GF254 Merck, $CHCl_3$, R_f 0.5) to give 0.3 g (62%) of **7**(Azo-Ole) as a reddish yellow powder: mp 128 → 137 °C; TLC (silica gel, $CHCl_3$) R_f 0.5; IR (KBr) ν(N—H) 3340 cm^{-1}, ν(C—H) 2920, 2850 cm^{-1}, ν(C=O, ester) 1740 cm^{-1}, ν(C=O, amide) 1640 cm^{-1}, n(C—O—C) + ν(C—F) 1170–1250 cm^{-1}.; ^{1}H-NMR (250 MHz, $CDCl_3$, 30 °C) δ 0.88 (t, 3H, –CH_3), 1.1–1.7 (m, 22H, –CH_2–), 1.82 (quintet, 2H, β-CH_2– to Ph—O–), 2.02 (m, 4H, —CH_2—C=), 2.19 (sextet, 1H, –CH– adjacent to the chiral carbon), 2.35 (sextet, 1H, –CH– adjacent to the chiral carbon), 2.4–2.6 (m, 6H, CF_2—CH_2– and OCO—CH_2–), 4.41 (octet, 2H, –CH_2—O), 4.55 (octet, 2H, –CH_2—O), 4.86 (sextet, 1H, CH–N), 7.10 (d, 1H, NH), 7.01 and 7.94 (dd, 4H, O—Ph—H), 7.94 (m, 4H, C(=O)—Ph—H). Anal. Calcd for $C_{56}H_{57}O_6NF_{34}$: C, 44.43; H, 3.79; N, 2.78. Found: C, 44.27; H, 3.89; N, 2.90.

1-Bromo-6-oxadodecane (16). 1-Hexanol (30.7 g, 0.30 mol) and freshly-cut Na (7.23 g, 0.32 mol) were mixed in dry THF (100 mL), and the mixture was refluxed for 3 h. The cooled suspension was added dropwise to a refluxing solution of 1,5-dibromopentane (103.5 g, 0.45 mol) in 100 mL of THF, and refluxing was continued for 5 h. After removal of the solvent in vacuo, the residues were diluted with 200 mL of $CHCl_3$ and washed with saturated aqueous NaCl solution (200 mL × 3). Solvent removal from the dried (Na_2SO_4) organic layer followed by distillation in vacuo gave 22.0 g of a colorless oil (bp 95–97 °C/1 mmHg). TLC (silica gel, $CHCl_3$/CH_3OH (4/1) R_f 0.9; ^{1}H-NMR (60 MHz, $CDCl_3$) δ 0.90 (t, 3H, –CH_3), 1.3–2.0 (m, 14H, –CH_2–), 3.37 (double t, 6H, O—CH_2– and Br—CH_2).

4-[(6-Oxadodecyl)oxy]benzoic Acid (17). Ethyl *p*-hydroxybenzoate (9.9 g, 60 mmol) and **16** (15.0 g, 60 mmol) were mixed with 200 mL of ethanol containing 4.7 g (70 mmol) of 85% KOH and the mixture was refluxed for 12 h. After the solution was cooled to room temperature, the precipitates were isolated. Solvent removal of the filtrate in vacuo gave 8.5 g of a colorless powder (mp 68 → 88 °C): TLC (silica gel, $CHCl_3$/CH_3OH (4/1)) R_f 0.9. This crude product was disolved in 200 mL of ethanol containing 10 mL of aqueous KOH (4.0 g, 60 mmol), and the mixture was refluxed for 5 h. Concentration of the reaction mixture in vacuo by 50% followed by cooling to room temperature produced colorless crystals (potassium salts). These were dissolved in water and acidified by concentrated HCl (pH 4). The precipitates were dried and recrystallized from petroleum ether to give 8.4 g (45%) of a colorless powder: mp 68 → 88 °C; TLC (silica gel, $CHCl_3$/CH_3OH (4/1)) R_f 0.8; IR (KBr) ν(C=O, COOH) 1690 cm^{-1}, ν(C—O—C) 1170, 1120 cm^{-1}; ^{1}H-NMR (60 MHz, $CDCl_3$) δ 0.87 (t, 3H, –CH_3), 1.3–2.0 (m, 14H, –CH_2–), 3.39 (t, 4H, O—CH_2–), 3.95 (t, 2H, PhO—CH_2–), 6.86 (d, 2H, aromatic), 7.85 (d, 2H, aromatic).

***N*-[[4-[(6-Oxadodecyl)oxy]phenyl]carbonyl]-*O*,*O*′-bis(1*H*,1*H*′,2*H*,2*H*′-perfluorodecyl)-L-glutamate (5).** **5** was synthesized from **10** (2.0 g, 1.6 mmol) and the acid chloride of **17** (1.0 g, 3.2 mmol) via a reaction with 17 mL of $SOCl_2$, in the same manner as the preparation of **7**. The yellowish, viscous solid was recrystallized twice from methanol, purified by chromatography on Kieselgel (Merck, mesh size 100–200, eluent $CHCl_3$, second elute was collected), and recrystallized again from methanol to give 0.84 g (39%) of a colorless powder: mp 66.5–67.5 °C; TLC (silica gel, $CHCl_3$) R_f 0.2; IR (KBr) ν(N—H) 3350 cm^{-1}, ν(C—H) 2920, 2850 cm^{-1}, ν(C=O, ester) 1738 cm^{-1}, ν(C=O, amide) 1640 cm^{-1}, ν(C—O—C) + ν(C—F) 1170–1250 cm^{-1}; ^{1}H-NMR (250 MHz, $CDCl_3$, 30 °C) δ 0.88 (t, 3H, –CH_3), 1.2–1.4 (m, 6H, –CH_2–), 1.5–1.8 (m, 6H, –CH_2–), 1.83 (quintet, 2H, β-CH_2– to Ph—O–), 2.14 (sextet, 1H, –CH– adjacent to the chiral carbon), 2.30 (sextet, 1H, –CH– adjacent to the chiral carbon), 2.4–2.6 (m, 6H, CF_2—CH_2– and OCO—CH_2–), 3.40 and 3.43 (dd, 4H, –CH_2—O—CH_2–), 4.00 (t, 2H, Ph—O—CH_2), 4.80 (sextet, 1H, CH—N), 6.92 and 7.76 (dd, 4H, Ph—H). Anal. Calcd for $C_{43}H_{41}O_7NF_{34}$: C, 38.84; H, 3.11; N, 1.05. Found: C, 38.98; H, 3.12; N, 1.08.

***N*-Octadecanoyl-*O*,*O*′-bis(1*H*,1*H*′,2*H*,2*H*′-perfluorodecyl)-L-glutamate (8).** Octadecanoyl chloride (0.3 g, 1.0 mmol), **10** (0.7 g, 0.5 mmol), and triethylamine (0.2 g, 2.0 mmol) were mixed in 30 mL each of $CHCl_3$ and 1,1,2-trifluoro-1,2,2-trichloroethane. The reaction mixture was stirred for 1 week at room temperature. The mixture was then washed with saturated aqueous NaCl (100 mL × 3), and the solvent was removed from the dried (Na_2SO_4) organic layer. The residue was recrystallized twice from toluene to give 0.45 g (61%) of a colorless powder: mp 111–113 °C; TLC (silica gel, $CHCl_3$) R_f 0.8; IR (KBr) ν(N—H) 3350 cm^{-1}, ν(C—H) 2920, 2850 cm^{-1}, ν(C=O, ester) 1740 cm^{-1}, ν(C=O, amide) 1650 cm^{-1}, ν(C—O—C) + ν(C—F) 1170–1250 cm^{-1}. Anal. Calcd for $C_{47}H_{49}O_7NF_{42}$: C ,37.49; H, 3.28; N, 0.93. Found: C, 37.47; H, 3.31; N, 0.97.

***N*-(Perfluoro-2,5,8-trimethyl-3,6,9-trioxadodecanoyl)-*O*,*O*′-didodecyl-L-glutamate (9).** This synthesis has been briefly reported.[71] Perfluoro-2,5,8-trimethyl-3,6,9-trioxadodecanoyl fluoride (1.3 g, 1.9 mmol, PCR Co.) in 60 mL each of dry THF and 1,1,2-trifluoro-1,2,2-trichloroethane was mixed with a solution of didodecyl glutamate hydrochloride (1.0 g, 1.9 mmol) and triethylamine (0.5 g, 4.9 mmol) in 60 mL of dry THF at room temperature. The mixture was refluxed for 5 days. After removal of the solvent in vacuo, the residues were mixed with $CHCl_3$ and washed with saturated aqueous NaCl solution. Evaporation of the dried (Na_2SO_4) organic layer followed by chromatography of the residue on silica gel (eluent $CHCl_3$) gave 0.83 g (40%) of **9** as colorless oil: mp 9.2 °C; TLC (silica gel/$CHCl_3$) R_f 0.7; IR (KBr) ν(N—H) 3350 cm^{-1}, ν(C—H)

2925, 2850 cm^{-1}, ν(C=O, ester, amide) 1740–1720 cm^{-1}, ν(C—F) 1150–1300 cm^{-1}; ^{1}H-NMR (400 MHz, $CDCl_3$, –20 °C, 10 mM) δ 0.88 (t, 6H, $-CH_3$), 1.2–1.4 (m, 36H, $-CH_2-$), 1.5–1.8 (m, 4H, β-CH_2– to –OC-(=O)), 2.10–2.20 (m, 1H, –CH– adjacent to the chiral carbon), 2.25–2.35 (m, 1H, –CH— adjacent to the chiral carbon), 2.35–2.55 (m, 4H, OCO—CH_2–), 4.07 and 4.17 (double t, 4H, $-CH_2$—O), 4.62 (quintet, 1H, CH—N), 7.89 and 8.00 (dd, 1H, NH). Anal. Calcd for $C_{41}H_{56}O_8NF_{23}$: C, 43.66; H, 5.00; N, 1.24. Found: C, 43.90; H, 5.00; N, 1.22.

Other Materials. Colorless, crude 1*H*,1*H*′,2*H*,2*H*′-perfluorodecan-1-ol was distilled in vacuo from a damp, brownish solid mixture (technical grade, gift of Asahi Glass Co. Ltd.) which contained $C_nF_{2n+1}CH_2CH_2OH$ (n = 4, 6, 8, 10, 12) as major ingredients. The pure alcohol (98% by gas chromatography) was obtained by additional distillation by using a column (90 × 2 cm) packed with small glass beads in vacuo (bp 70–74 °C/2 mmHg; mp 41–42 °C).

Chlorocyclohexane (Aldrich, 99%) was distilled twice. Benzene and toluene (Kishida Chemical Co., spectrophotomeric grade) were distilled from sodium wire. Methanol in the reagent grade was distilled from Mg/iodine. Chloroform (reagent grade) was free of ethanol and water. Other solvents in Table 1 were chromatographic grades (Aldrich and Kishida) and were used as supplied. Lead(II) bis(acetylacetonate) used for negative staining was purchased from Dojindo Laboratories (Japan) and was used without further purification.

Methods. Amphiphiles **3** (Ole), **6** (Phe-Ole), and **7** (Azo-Ole) were readily dissolved in benzene and toluene at 40–60 °C. They gave translucent dispersions in chlorocyclohexane (up to 20 mM) by sonication at 70–80 °C with Bransonic Cell Disruptor 185 (sonic power 30, 1 min). The dispersions were aged at room temperature for more than overnight prior to physicochemical measurements. Transmission electron microscopy (TEM) was conducted on a Hitachi H-600 instrument by the negative post staining method. The bilayer dispersions were cautiously spread over carbon-coated Cu meshes at about 10 °C for several times and dried. Then a hot saturated solution of $Pb(acetylacetonato)_2$ in methanol was dropped as a negative staining agent and dried in vacuo. The Cu meshes were subjected to TEM observation with an acceleration voltage of 75 kV and magnifications of 10 000–60 000. Optical microscopic observation was done through an Olympus BH 1000 with an ultraviolet light. Differential scanning calorimetry (DSC) was conducted on a Seiko SSC-5200 instrument. The dispersions (20 mM, 56 μL) were sealed in Ag-sample pans. The solvent was used as a control sample. DSC thermograms were scanned at a rate of +1 °C/min from –10 to +100 °C several times. The molecular weights of the dispersions (2 mM) were determined at 70 °C by vapor pressure osmometry using a Corona Model 117 molecular weight apparatus. Circular dichroism (CD) measurements were carried out on a JASCO J-40AS spectropolarimeter with a 0.1-cm cell. Infrared spectra were acquired with a Nicolet 710 FT-IR spectrometer. The dispersions (20 mM) were placed in a KBr liquid cell (0.5-mm width) and mounted on a homemade constant-temperature cell holder at 15 and 40 °C (±2 °C). The spectra were obtained by running 32 sample scans against 32 solvent scans at 2-cm^{-1} resolution. The equilibrium surface tension was measured on a Shimadzu ST-1 tensiometer using a Wilhelmy plate (sandblasted glass, 1.5 × 1.0 cm^2) with an experimental error of ±0.5 mN/m. The glass plate was sufficiently wetted with chlorocyclohexane to follow the change in surface tension. The temperature was kept constant within 0.1 °C using a constant-temperature cell holder. The instrument was calibrated against surface tensions of pure solvents. The air/solvent surface possessing a Wilhelmy plate was made to equilibrate by keeping at temperatures of measurement for at least 2 h prior to each measurement. The measured surface tension of chlorocyclohexane agreed with its reported value (31.9 mN/m at 18 °C) with an error of ±0.5 mN/m.

Acknowledgment. Prof. Thomas W. Healy (University of Melbourne, Australia) and Dr. Neil Furlong (CSIRO, Australia) pointed out the importance of the thermodynamic treatment of the data in Figures 6 and 7. Prof. Kinsi Motomura and his colleagues (Kyushu University) kindly helped us to understand their theory.[53,54] We also thank Mr. Hideaki Horiuchi for skillful preparation of a home-designed distillation glass column and the Asahi Glass Co. Ltd. for providing fluorocarbon materials.